



RESEARCH  
PROGRAM  

---

DIGITAL  
FOR EXASCALE

Workshop "Artificial Intelligence for HPC@Exascale"

Image Analysis/Scaling-up Data  
& Data Analysis/Inferences

PARIS – Thursday October 3<sup>rd</sup>, 2024

# Deep learning based approach in imaging radiometry by aperture synthesis: from the **idea** to the **implementation**



UMR5126  
18 av. Edouard Belin  
31400 Toulouse

Eric ANTERRIEU  
& the SMOS team

# The SMOS space mission

## ➤ A long story

- 1983-1984: statement of requirements
- 1983-1986: seek & explore solutions
- 1987-1988: theoretical solution
- 1988-1991: practical solution
- 1991-1997: mission proposal
- 1997-1999: mission acceptance & initialization
- 1999-2009: payload manufacturing, assembly & tests
- 2009-2010: launch (02-Nov-2009) & commissioning phase
- 2010-.....: operational phase

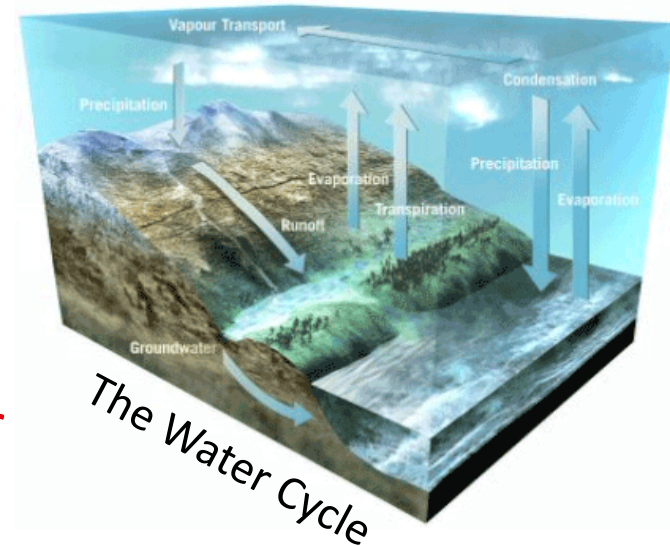
# The SMOS space mission

## ➤ The context

ESA's **Soil Moisture and Ocean Salinity** (SMOS) mission has been designed to observe both soil moisture over the Earth's landmasses and salinity over the oceans from space.

SM data are urgently required for hydrological studies and data on OS are vital for improving our understanding of ocean circulation patterns.

*SMOS was a direct response to the current lack of global observations of SM and OS.*



# The SMOS space mission

## ➤ The concept

A novel instrument has been especially developed with the objective to demonstrate the use of a **Microwave Imaging Radiometer by Aperture Synthesis** for imaging SM and OS by “capturing” images of emitted microwave radiation Tb in the “protected” L-band (1400-1427 MHz).

*SMOS was the first attempt to apply to Earth remote sensing the concept of aperture synthesis initially developed by radio astronomers.*



VLA (1970's)

# The SMOS space mission

## ➤ The concept

A novel instrument has been especially developed with the objective to demonstrate the use of a **Microwave Imaging Radiometer by Aperture Synthesis** for imaging SM and OS by “capturing” images of emitted microwave radiation Tb in the “protected” L-band (1400-1427 MHz).

*SMOS was the first attempt to apply to Earth remote sensing the concept of aperture synthesis initially developed by radio astronomers.*



CBI (1990's)



# The SMOS space mission

## ➤ The concept

A novel instrument has been especially developed with the objective to demonstrate the use of a **Microwave Imaging Radiometer by Aperture Synthesis** for imaging SM and OS by “capturing” images of emitted microwave radiation  $T_b$  in the “protected” L-band (1400-1427 MHz).

*SMOS was launched on 2nd November 2009 and although designed for a five-year mission, it is still operational after more than 15 years in orbit.*



SMOS (2000's)

# The SMOS space mission

## ➤ The instrument

The single payload of SMOS is MIRAS, a **Microwave Imaging Radiometer by Aperture Synthesis**, operating in full-pol mode in the “protected” L-band (1400-1427 MHz).

MIRAS is a **Y-shaped array** equipped with **69 elementary antennas** provides inter-ferometric measurements, 3 (of them) operating also as reference radio-meters to provide measurements of the average brightness temperature of the scene under observation.



SMOS (2000's)

# Aperture synthesis imaging

## ➤ Arrays with connected antennas

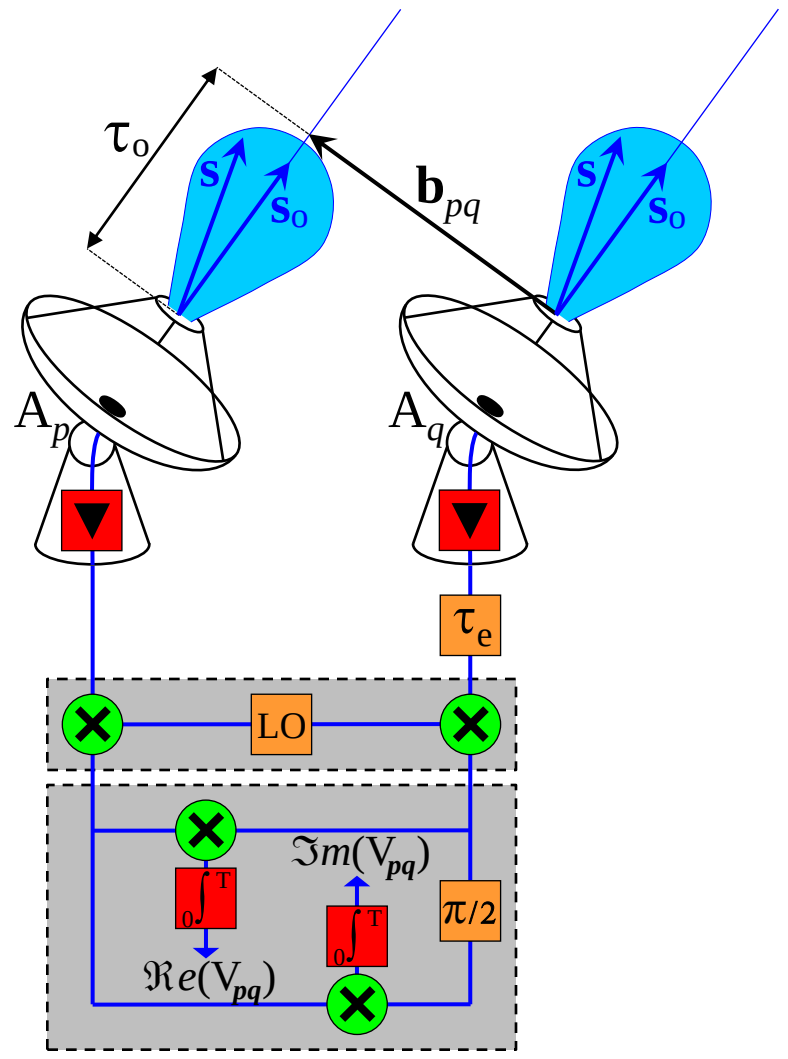
The **radio signals** received by the two antennas are **sampled** and directly **transmitted** via links to the **correlation unit** which combines them to produce **interference fringes** in **real time**.



Cosmic Background Imager



Very Large Array

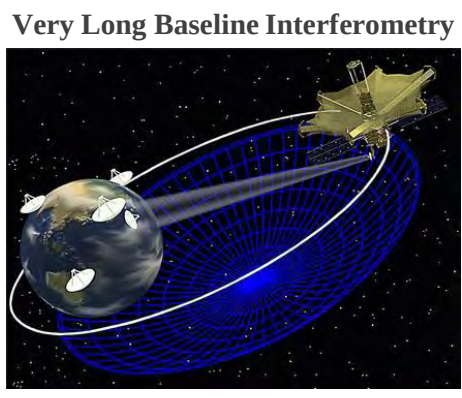
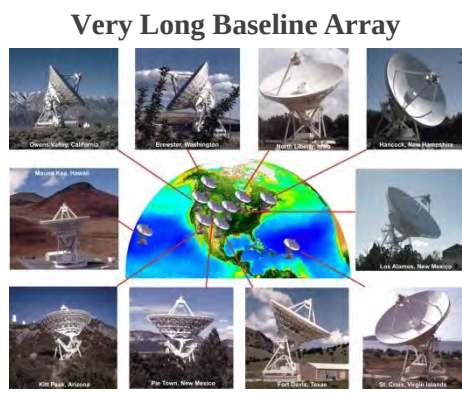
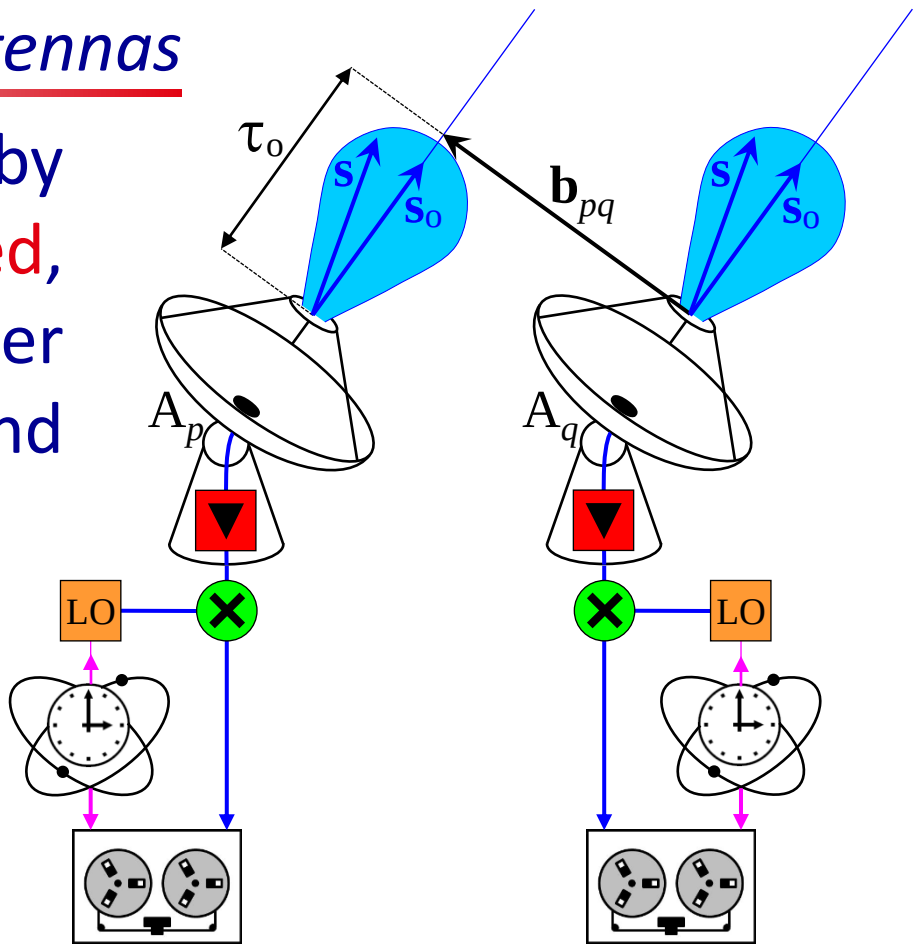




# Aperture synthesis imaging

## ➤ Arrays with unconnected antennas

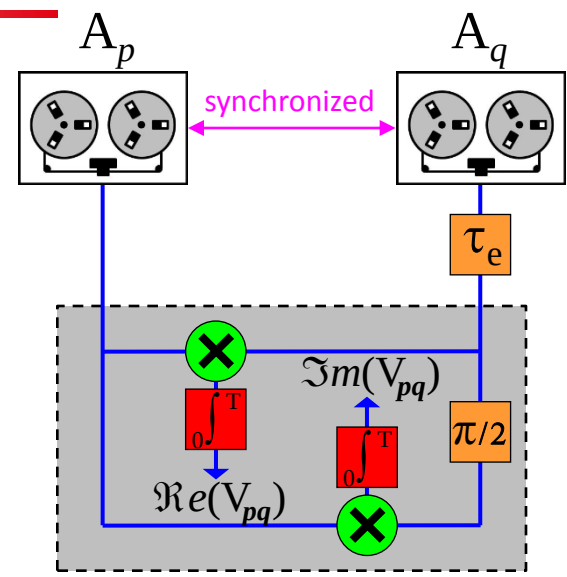
1) The **radio signals** received by the two antennas are **sampled, recorded** alongside together with an **accurate time base** and then **stored** on a media...



# Aperture synthesis imaging

## ➤ Arrays with unconnected antennas

- 1) The **radio signals** received by the two antennas are **sampled, recorded** alongside together with an **accurate time base** and then **stored** on a media.
- 2) At a later time, at the location of a **correlation unit**, the data are **synchronized**, then **played back** together and combined just like if they were coming in real time from the two antennas.

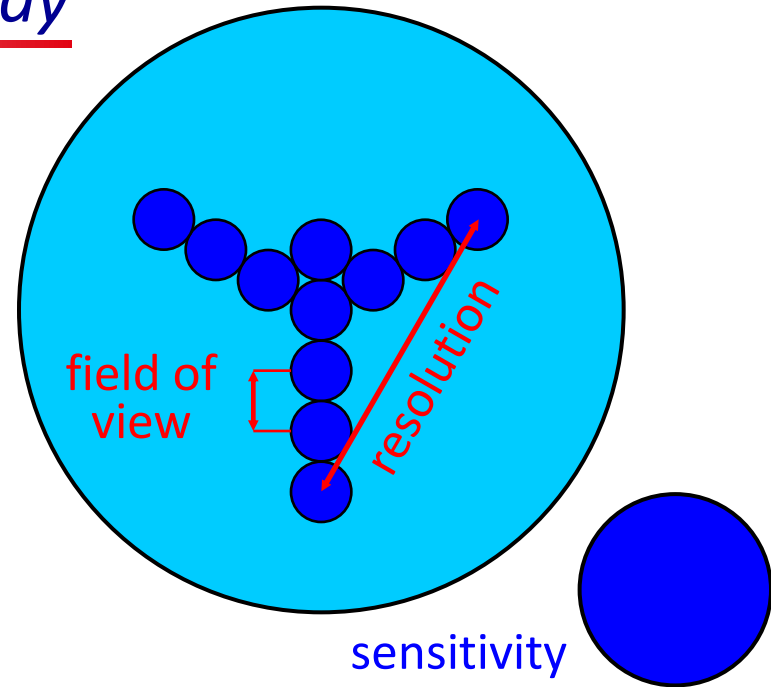


VLBI correlation unit hosted by the Max Planck Institute for Radio Astronomy

# Aperture synthesis imaging

## ➤ Key parameters of an antenna array

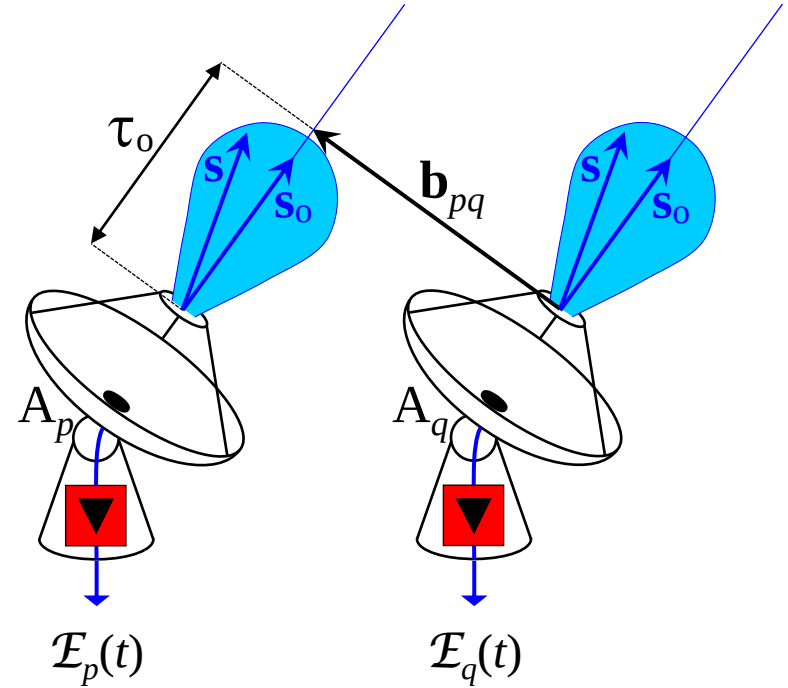
- 1) **Field of view**: the extent of the observed scene that is synthesized by the instrument (with the aid of the computer).
- 2) **Angular resolution**: the ability to distinguish small details of the observed scene (estimated with Rayleigh / Schuster / Sparrow criterions of PSF, not of PSF2 !).
- 3) **Radiometric sensitivity**: the smallest temperature deviation that can be discerned by the instrument.



# Aperture synthesis imaging

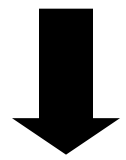
## ➤ Complex visibilities

Whether the antennas are connected or not, interferometer measurements are obtained by **cross-correlating** the signals  $\mathcal{E}_p(t)$  and  $\mathcal{E}_q(t)$  collected by **pairs of spatially separated antennas**  $A_p$  and  $A_q$  which have **overlapping fields of view**, yielding samples of the **spatial coherence function**  $V_{pq}$  (also termed **complex visibilities**) of the brightness temperature distribution  $T_b$  of the scene under observation for the angular frequency  $\mathbf{u}_{pq} = \mathbf{b}_{pq}/\lambda_o$ .



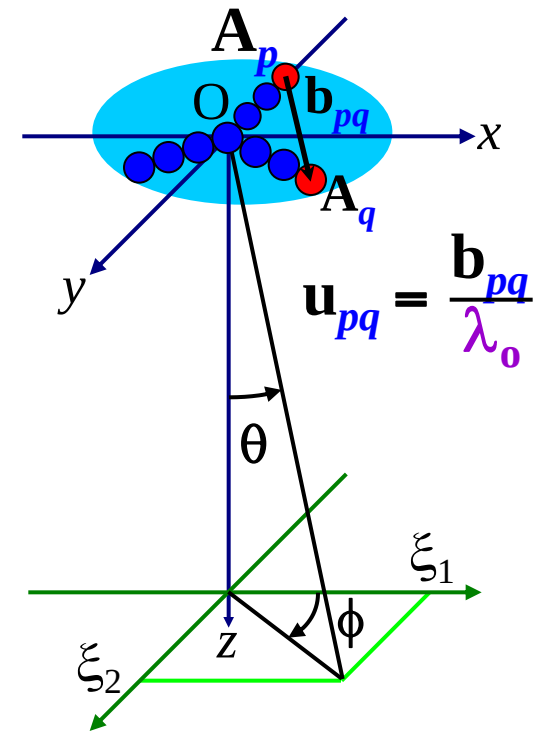
## ➤ Van Cittert – Zernike theorem revisited

$$\mathbf{V}_{pq} \propto \frac{1}{\sqrt{\Omega_p \Omega_q}} \iint_{\|\xi\| \leq 1} \mathcal{F}_p(\xi) \mathcal{F}_q^*(\xi) [\mathbf{T}_b(\xi) - \mathbf{T}_{rec}] \tilde{\mathbf{r}}_{pq}(t) \frac{e^{-2j\pi \mathbf{u}_{pq} \cdot \xi}}{\sqrt{1 - \|\xi\|^2}} d\xi$$



$$\mathbf{V} = \mathbf{G} \mathbf{T}$$

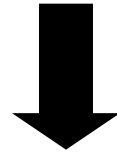
- $\mathcal{F}$  : antenna voltage pattern
- $\mathbf{T}_{rec}$  : receivers temperature
- $\tilde{\mathbf{r}}$  : fringe washing function ( $t = \mathbf{u}_{kl} \cdot \xi / f_o$ )
- $\mathbf{V}$  : complex visibilities
- $\mathbf{T}_b$  : brightness temperature ( $\mathbf{T}(\xi) = \mathbf{T}_b(\xi) - \mathbf{T}_{rec}$ )





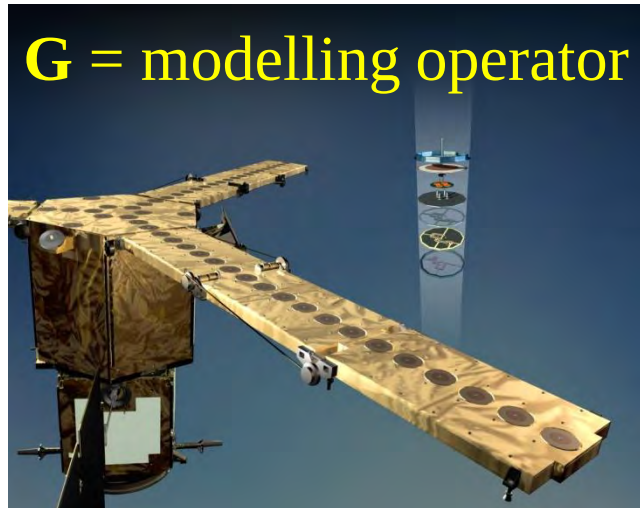
➤ Van Cittert – Zernike theorem revisited

$$V_{pq} \propto \frac{1}{\sqrt{\Omega_p \Omega_q}} \iint_{\|\xi\| \leq 1} \mathcal{F}_p(\xi) \mathcal{F}_q^*(\xi) [\mathbf{T}_b(\xi) - \mathbf{T}_{rec}] \tilde{\mathbf{r}}_{pq}(t) \frac{e^{-2j\pi \mathbf{u}_{pq} \cdot \xi}}{\sqrt{1 - \|\xi\|^2}} d\xi$$



$$\mathbf{V} = \mathbf{G} \mathbf{T}$$

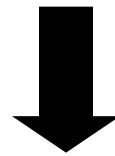
**G = modelling operator**



## ➤ Dual polarization

$$V_{pq}^x \propto \frac{1}{\sqrt{\Omega_p \Omega_q}} \iint_{\|\xi\| \leq 1} \left[ C_p^x(\xi) C_q^{x*}(\xi) [T_b^x(\xi) - T_{rec}] + X_p^x(\xi) X_q^{x*}(\xi) [T_b^y(\xi) - T_{rec}] \right] \tilde{r}_{pq}(t) \frac{e^{-2j\pi \mathbf{u}_{pq} \cdot \xi}}{\sqrt{1 - \|\xi\|^2}} d\xi$$

$$V_{pq}^y \propto \frac{1}{\sqrt{\Omega_p \Omega_q}} \iint_{\|\xi\| \leq 1} \left[ X_p^y(\xi) X_q^{y*}(\xi) [T_b^x(\xi) - T_{rec}] + C_p^y(\xi) C_q^{y*}(\xi) [T_b^y(\xi) - T_{rec}] \right] \tilde{r}_{pq}(t) \frac{e^{-2j\pi \mathbf{u}_{pq} \cdot \xi}}{\sqrt{1 - \|\xi\|^2}} d\xi$$



$$\mathbf{V} = \mathbf{G} \mathbf{T}$$

$$\mathbf{V} = \begin{pmatrix} V^x \\ V^y \end{pmatrix}$$

$$\mathbf{G} = \begin{pmatrix} G^{xx} & G^{xy} \\ G^{yx} & G^{yy} \end{pmatrix}$$

$$\mathbf{T} = \begin{pmatrix} T^x(\xi) \\ T^y(\xi) \end{pmatrix} = \begin{pmatrix} T_b^x(\xi) - T_{rec} \\ T_b^y(\xi) - T_{rec} \end{pmatrix}$$

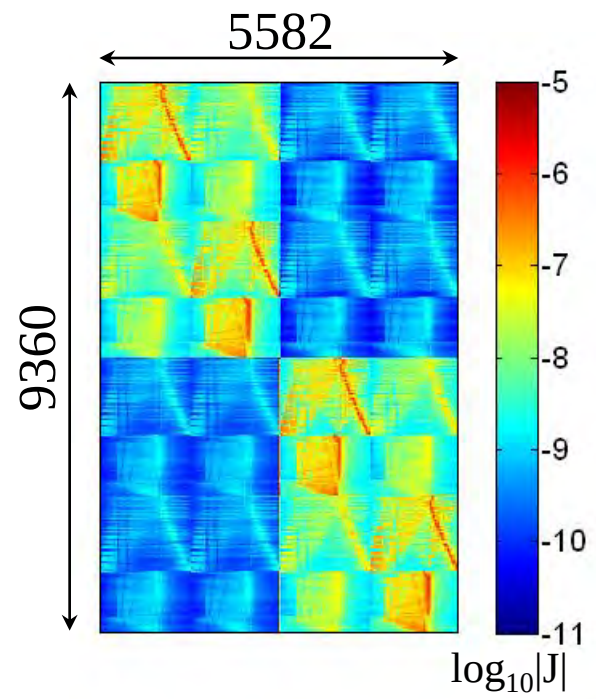
# Regularized inversion

## Dual polarization

$$\begin{pmatrix} \mathbf{T}_r^x \\ \mathbf{T}_r^y \end{pmatrix} = \begin{pmatrix} \mathbf{U}^* \mathbf{Z} & \mathbf{0} \\ \mathbf{0} & \mathbf{U}^* \mathbf{Z} \end{pmatrix} \begin{pmatrix} \mathbf{J}^{xx} & \mathbf{J}^{xy} \\ \mathbf{J}^{yx} & \mathbf{J}^{yy} \end{pmatrix}^+ \left[ \begin{pmatrix} \mathbf{V}^x \\ \mathbf{V}^y \end{pmatrix} - \begin{pmatrix} \mathbf{G}^{xx} & \mathbf{G}^{xy} \\ \mathbf{G}^{yx} & \mathbf{G}^{yy} \end{pmatrix} \begin{pmatrix} \tilde{\mathbf{T}}^x \\ \tilde{\mathbf{T}}^y \end{pmatrix} \right] + \begin{pmatrix} \tilde{\mathbf{T}}^x \\ \tilde{\mathbf{T}}^y \end{pmatrix}$$

*numerical implementation in ground segment*

69 antennas  
dual polarisation  
( $\mathbf{J} \sim 400$  Mbytes)

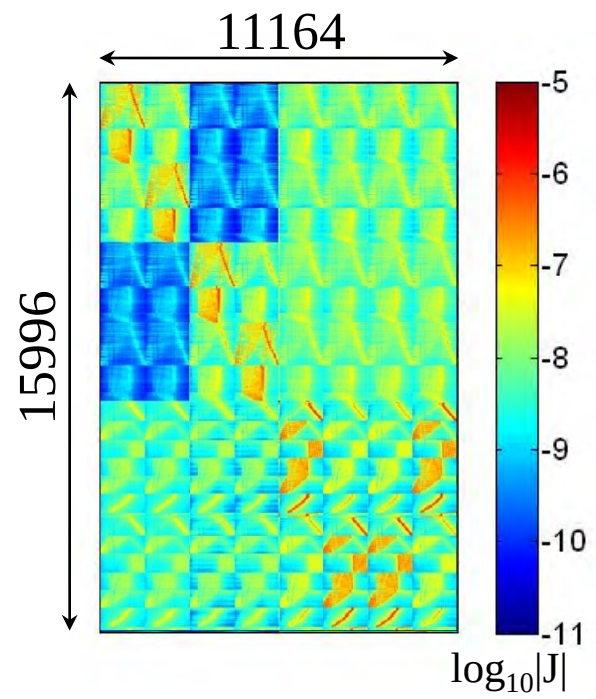


➤ *Full polarization*

$$\begin{pmatrix} T_r^x \\ T_r^y \\ T_r^3 \\ T_r^4 \end{pmatrix} = \dots \begin{pmatrix} V^x \\ V^y \\ V^{xy} \end{pmatrix} \dots$$

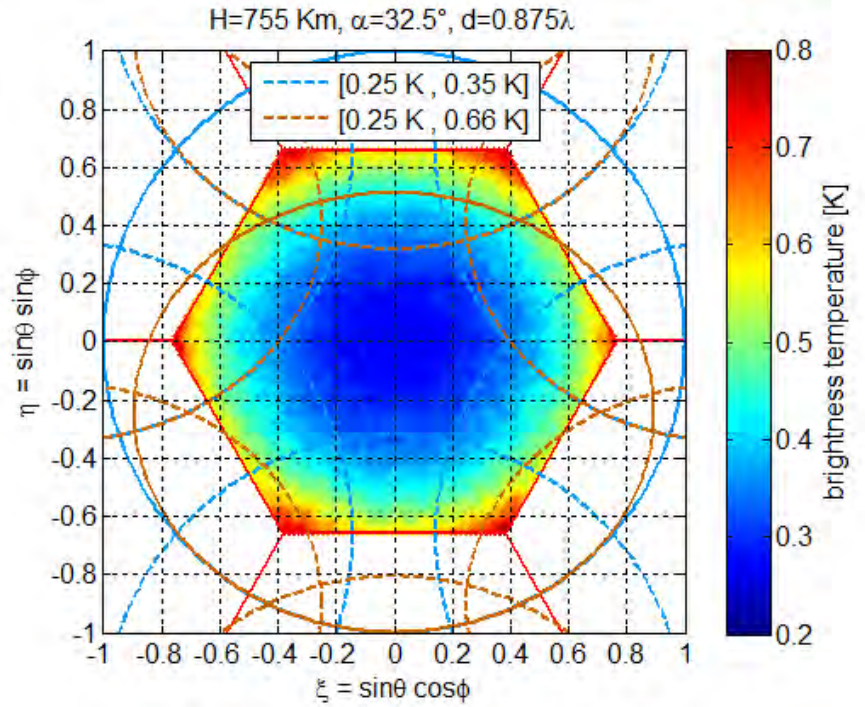
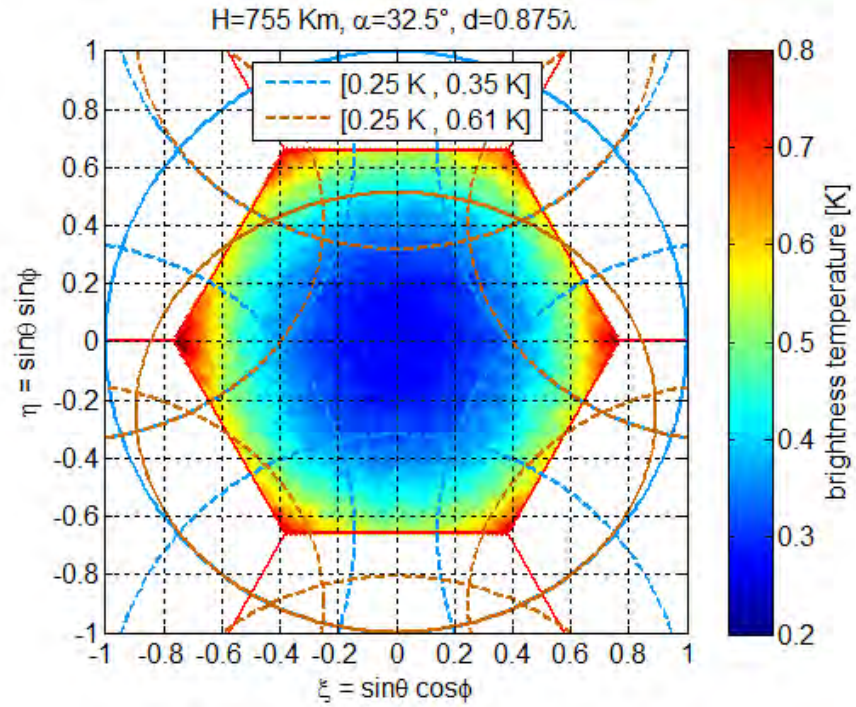
*numerical implementation in ground segment*

69 antennas  
full polarisation  
(**J** ~ 1.3 Gbytes)



# Illustrations & performances

➤ *Noise propagation:  $\Delta V = N(0, \sigma^2)$  with  $\sigma = 0.01 K$*

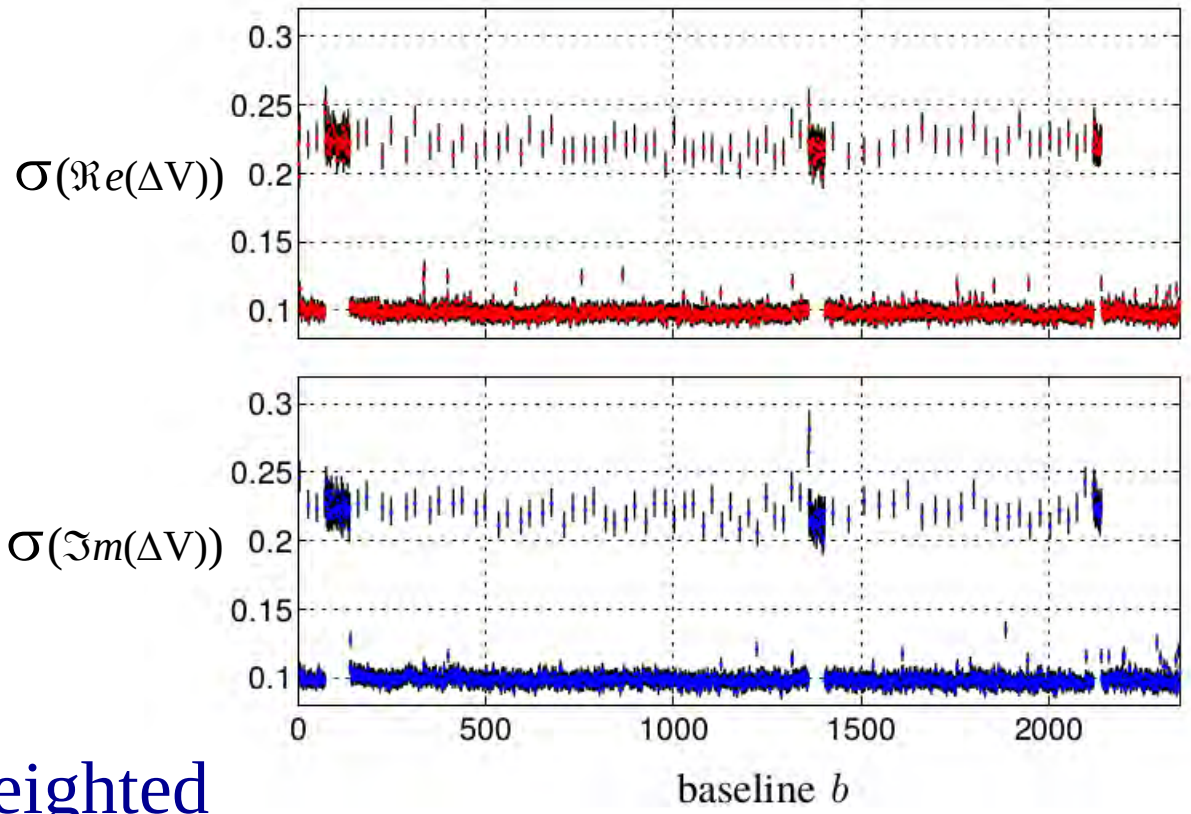


Amplification factor:  $\times 25$  (num. simul.)  
(boresight)  $\times 25$  (radio. theory)



# Illustrations & performances

## ➤ Noise statistics: heteroscedastic vs. homoscedastic



0.1 K error on  $T_b$  may induce 0.2-0.3 PSU error in retrieved SSS

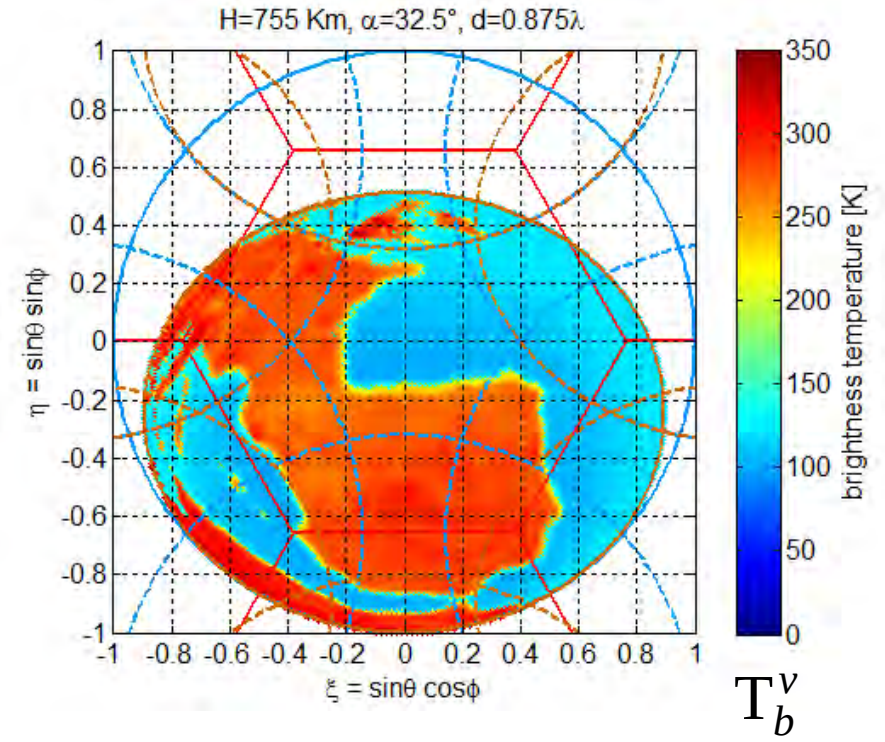
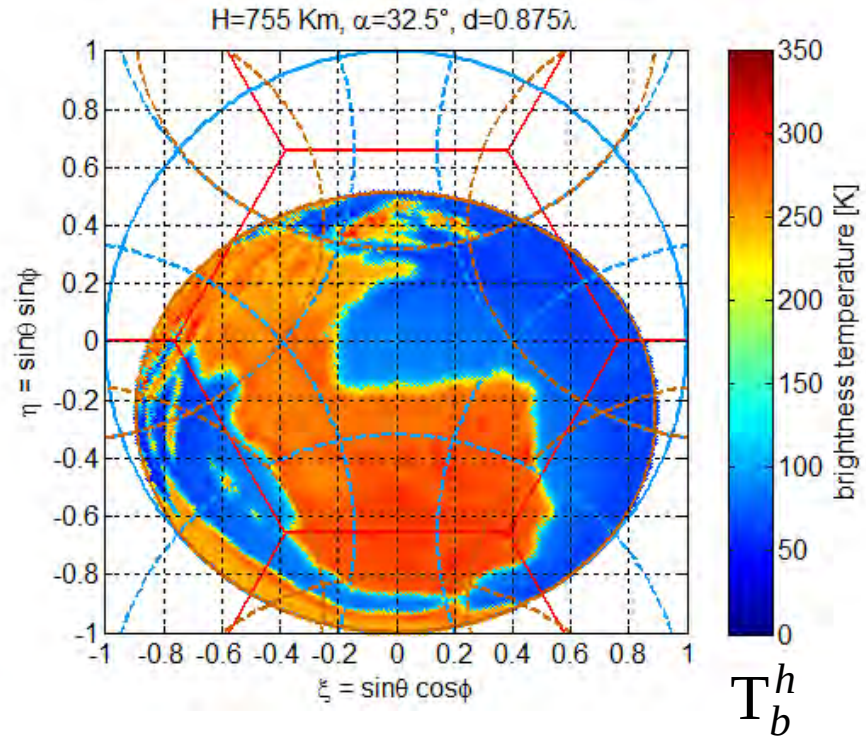
Weighted  
vs. inversion  
Standard

$\Rightarrow$  radiometric sensitivity:

2.3 K vs. (-8%)  
2.5 K

# Illustrations & performances

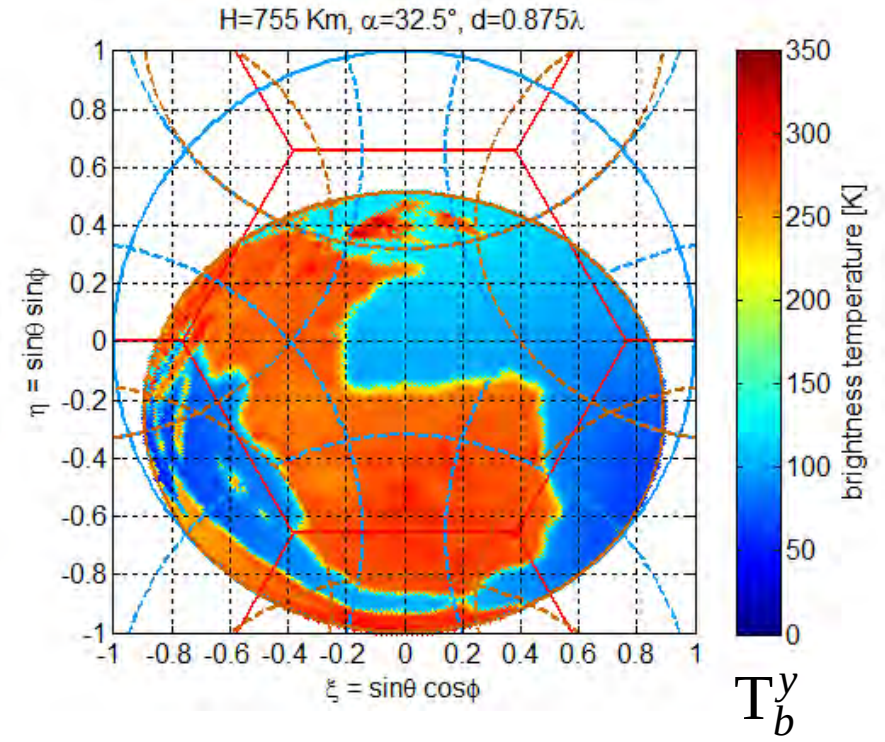
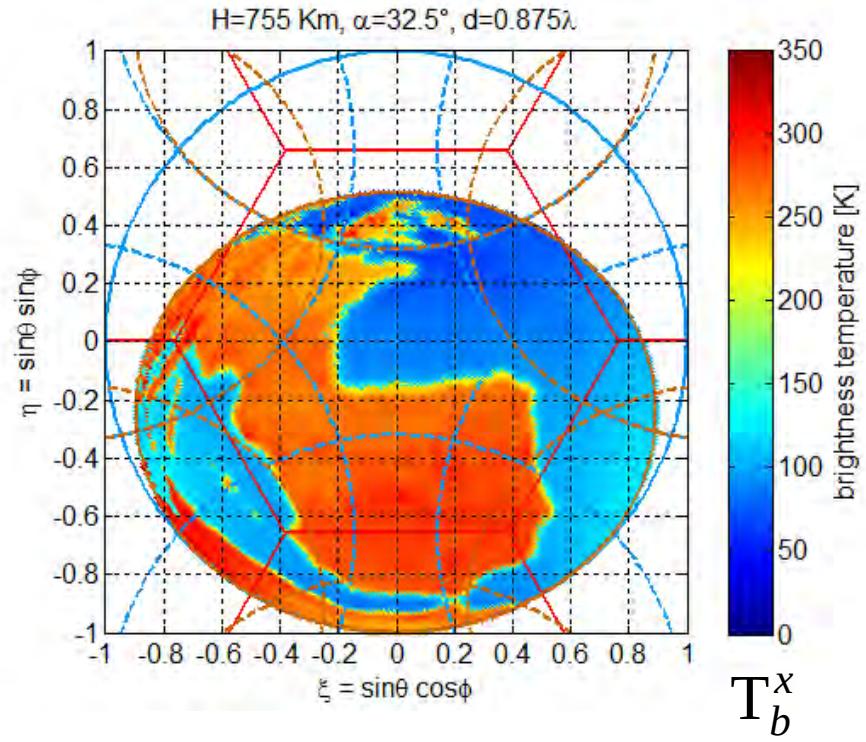
## ➤ Observed scene: H & V





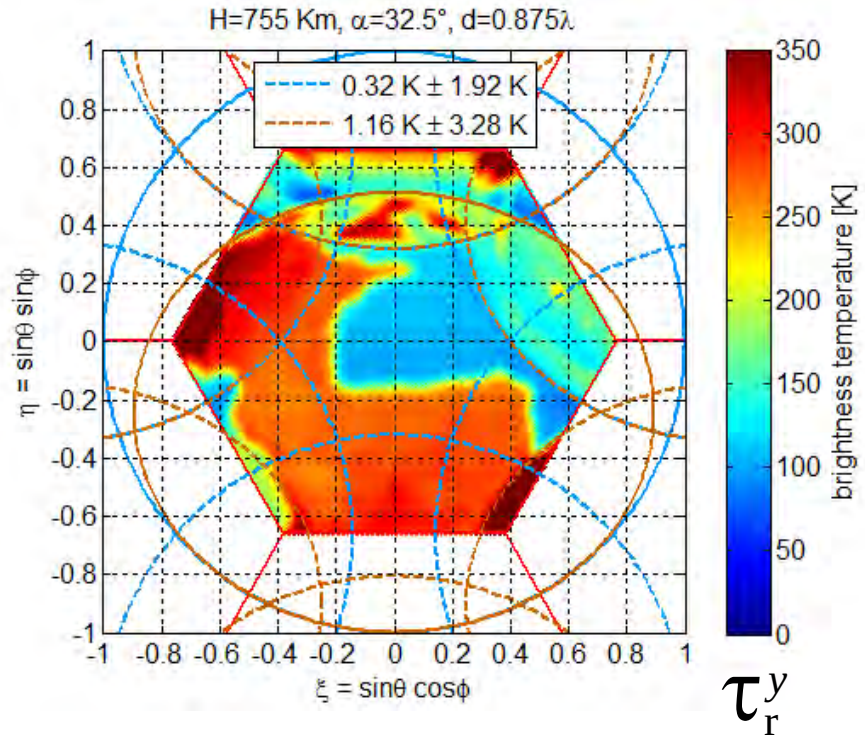
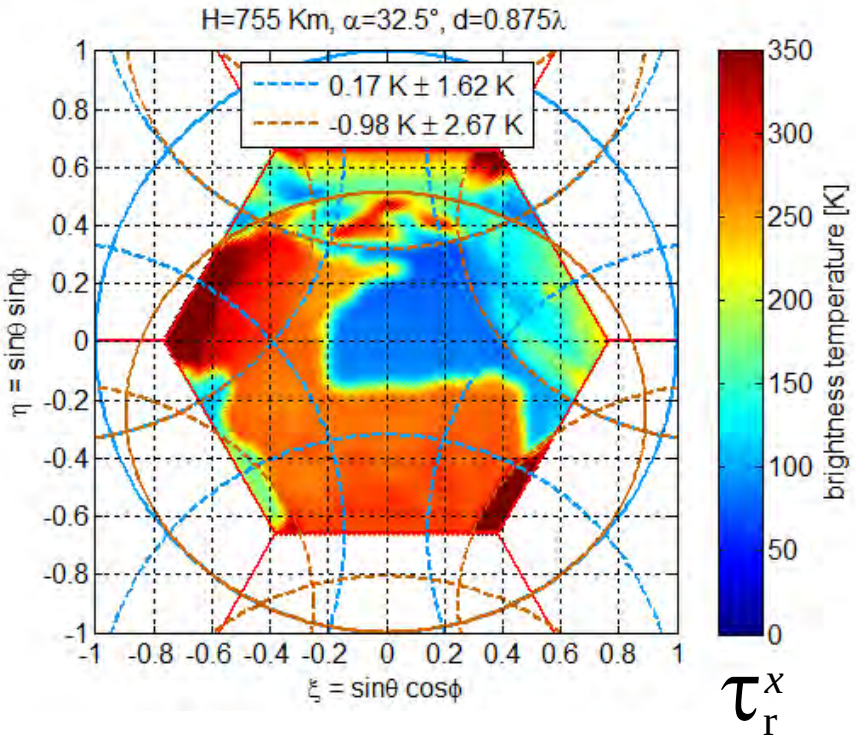
# Illustrations & performances

## ➤ Observed scene: X & Y



# Illustrations & performances

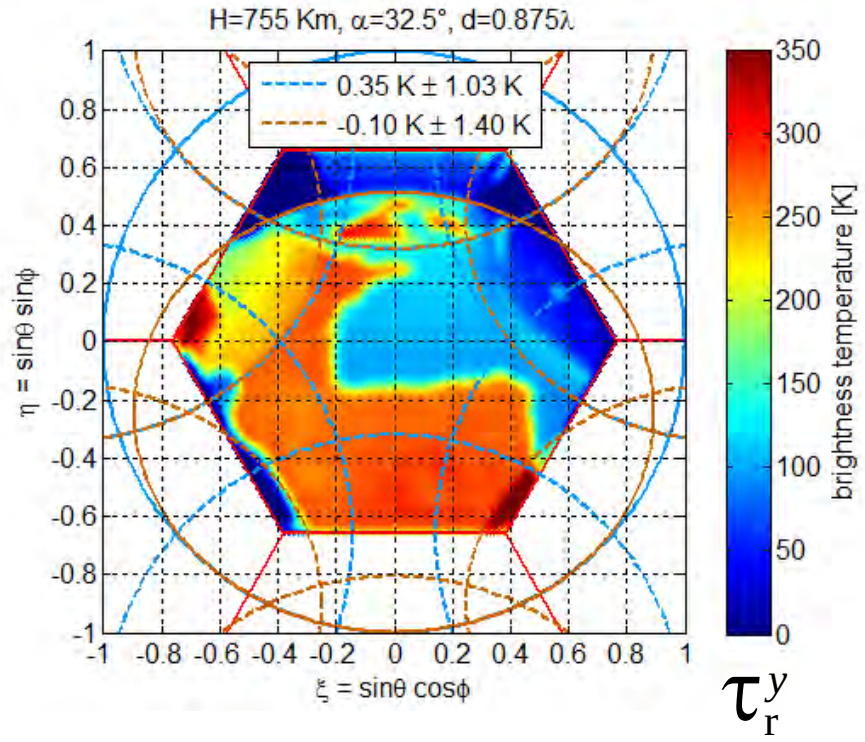
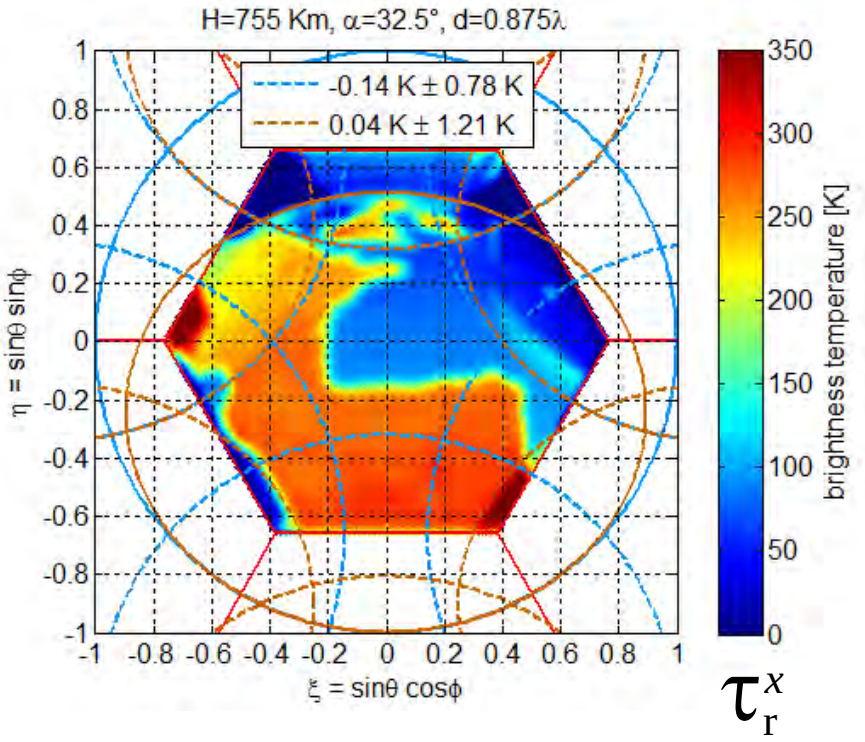
## ➤ Standard inversion





# Illustrations & performances

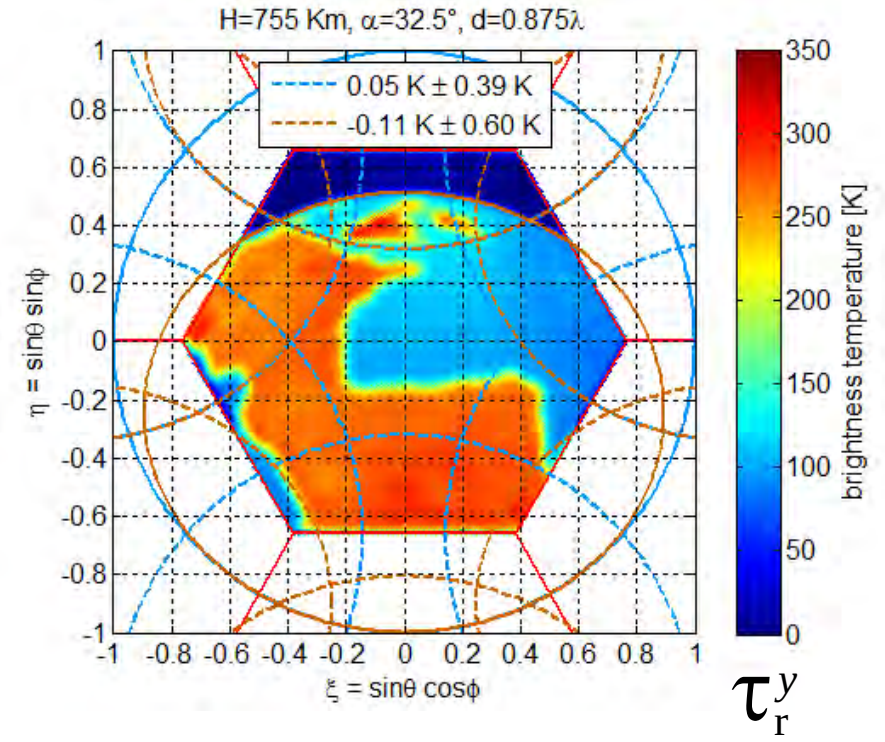
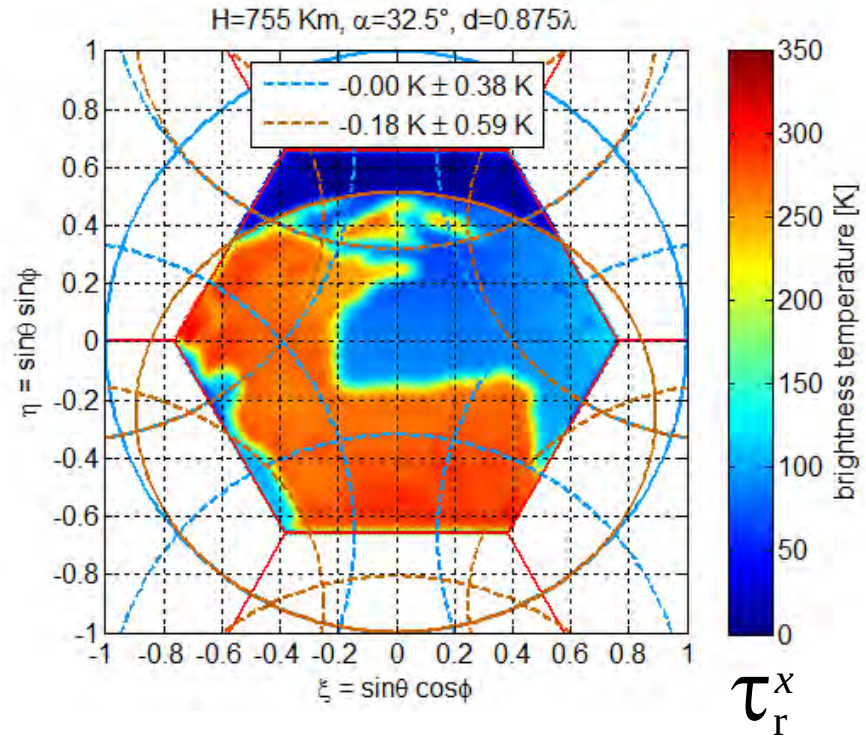
## Differential inversion with $\tilde{T}(t_{sky}, t_{earth})$





# Illustrations & performances

## Differential inversion with $\tilde{T}(t_{sky}, t_{land}, t_{ocean})$



# A co-design approach

## ➤ Participatory design (from Scandinavia)

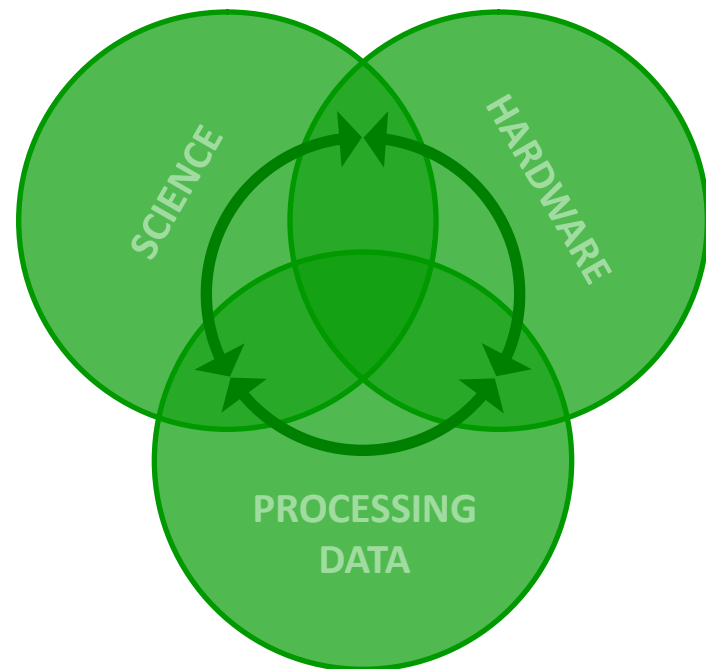
Co-design (or co-operative design) is an approach to design attempting to actively involve all stakeholders (e.g. **employees, partners, customers, citizens, end-users**) in the design process to help ensure the result meets their **needs** and is **usable** and **marketable**. All the participants are invited to cooperate during the several stages of an innovation process.



# A co-design approach

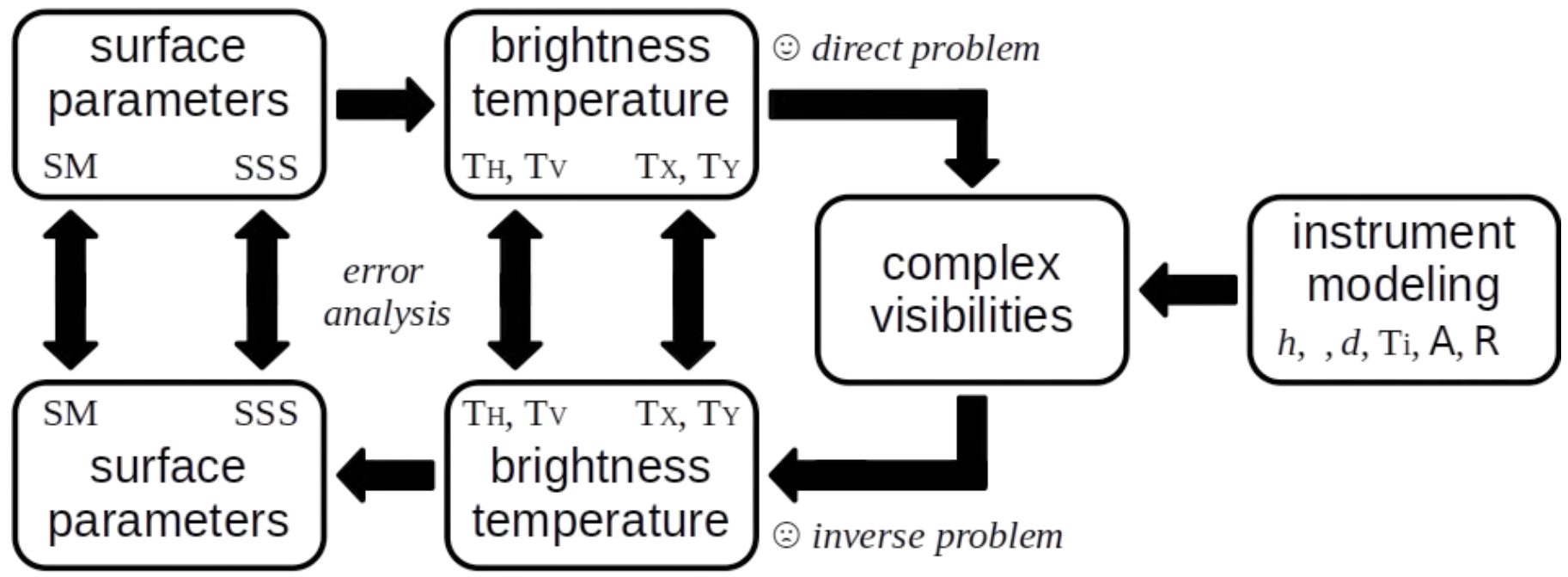
## ➤ Participatory design (in scientific instrumentation)

Time consuming **end-to-end simulations** involving **engineers**, **scientists** and **end-users** actively collaborating are playing an ongoing role for assessing the **sensitivity** and the **robustness** of mission performances to **driving parameters**, to **instrument errors** and **noises** as well as to **data processing** and analysis.



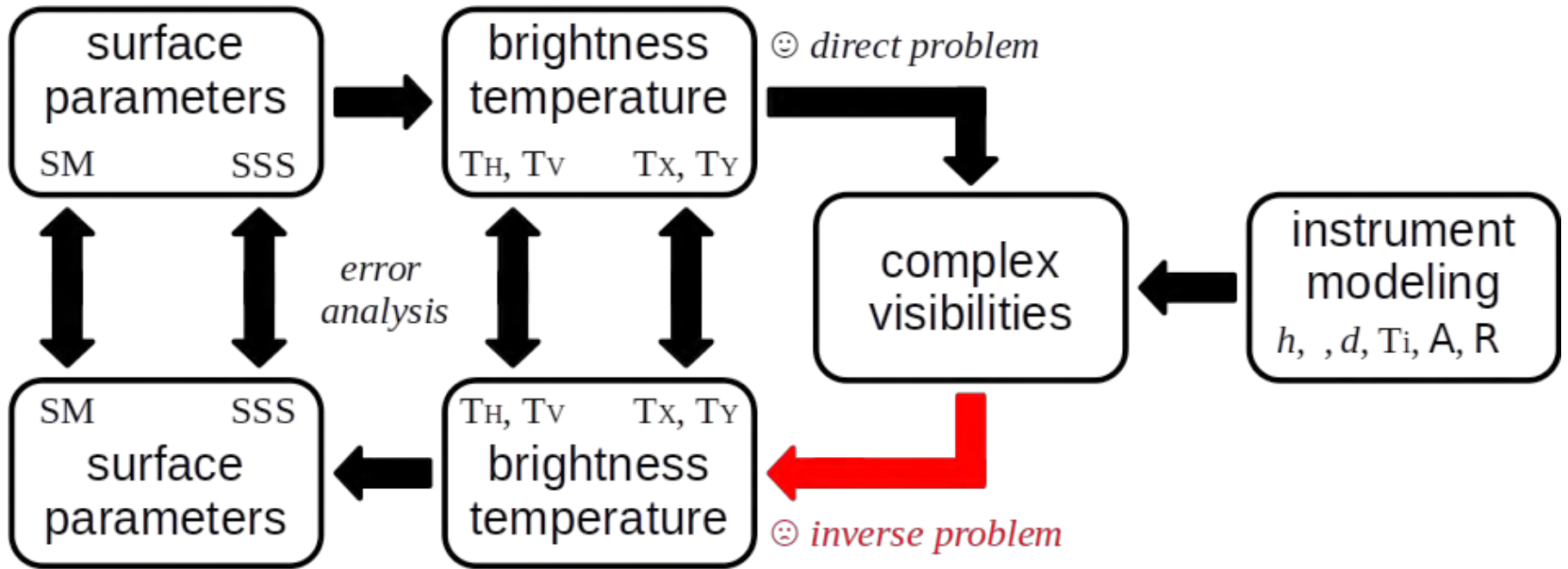
# A co-design approach

➤ An end-to-end simulator for participatory design



# A co-design approach

## ➤ An end-to-end simulator for participatory design





# A deep-learning approach

## ➤ Building dataset: numerical simulations

Dual-polarization {T,V} simulated from monthly SMOS L3.  
One snapshot {T,V} = 34087  $T_{ij}$  (23042 earth + ~~11045 sky~~)  
+ 4695  $V_{pq}$  ( $69 \times (69-1) + 3$ )

Only 1 snapshot every 12 sec, first 3 days of every 12 months,  
Year 2012 {T,V} = 332791 snapshots (166557  $\uparrow$  + 166234  $\downarrow$ )  
 $\approx$  70 Gbytes per polarization

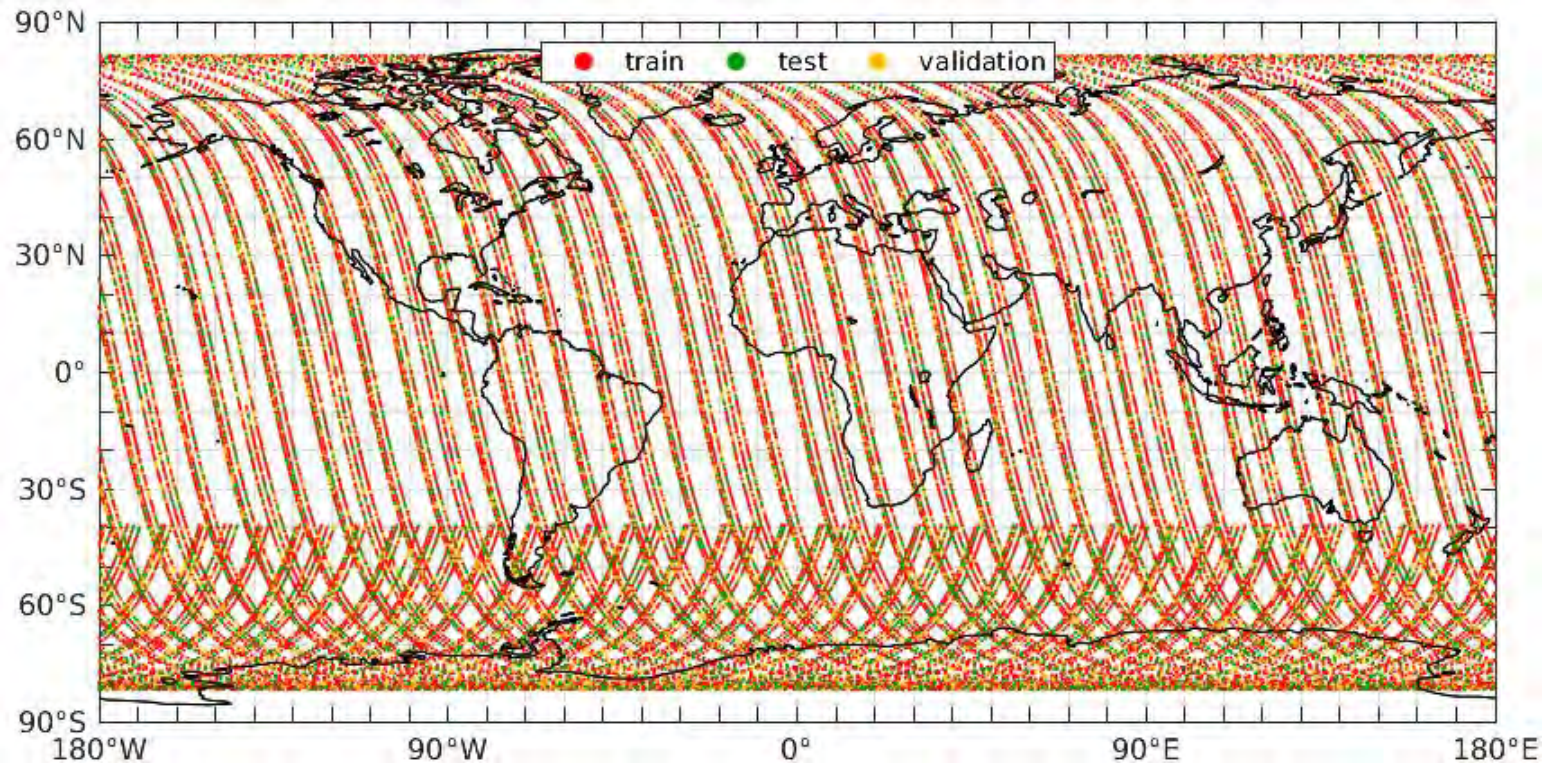
{T,V} dataset  $\approx$  140 Gbytes

$\Rightarrow$  only  $\uparrow$  snapshots in X-polarization ( $\approx$  35 Gbytes)

# A deep-learning approach

## ➤ Splitting dataset

60% (training) + 20% (validation) + 20% (testing)



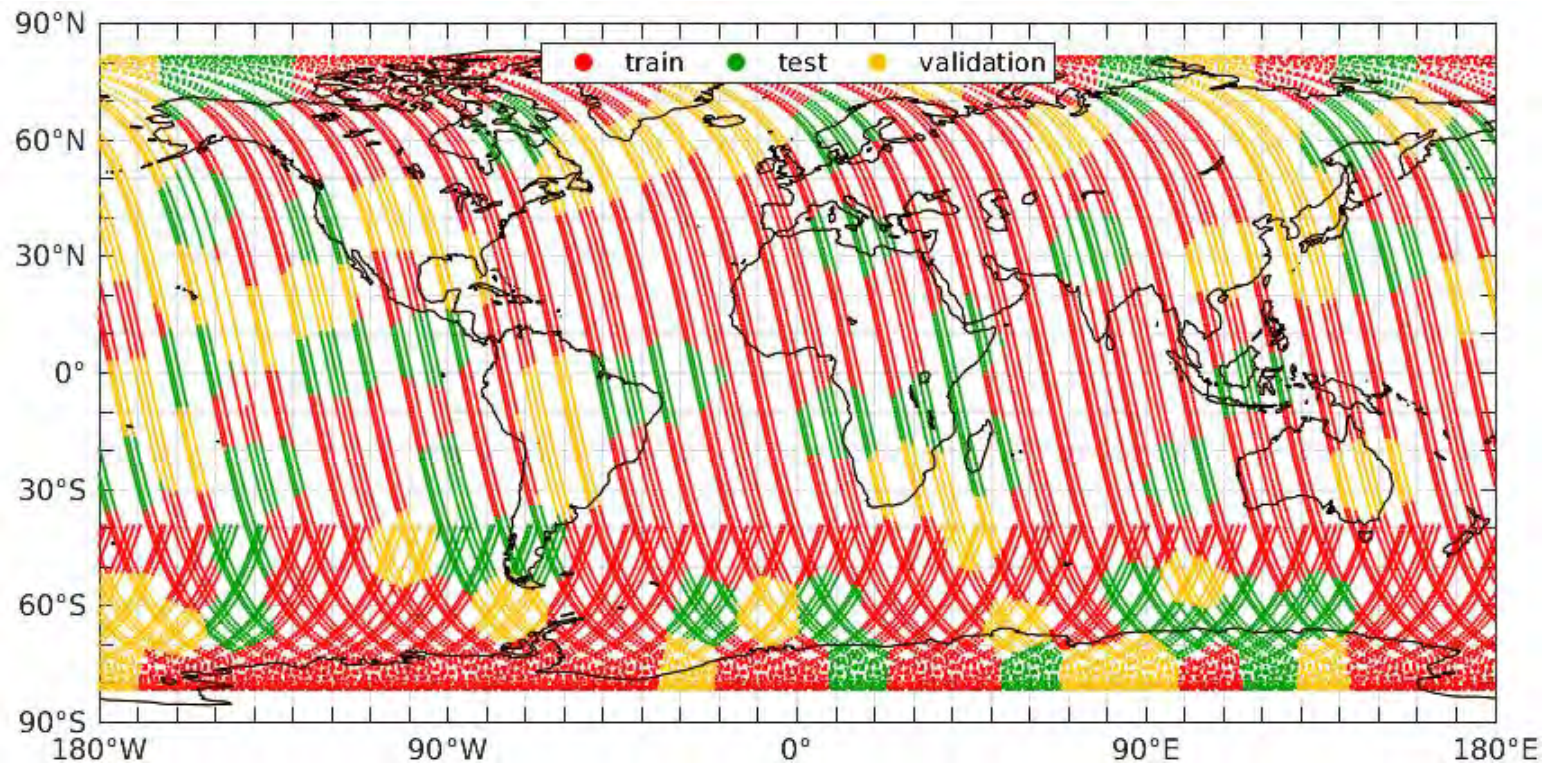
random split (risk of similar {T,V} for train/valid/test)



# A deep-learning approach

## ➤ Splitting dataset

60% (training) + 20% (validation) + 20% (testing)



K-means split (over-training risk reduced)



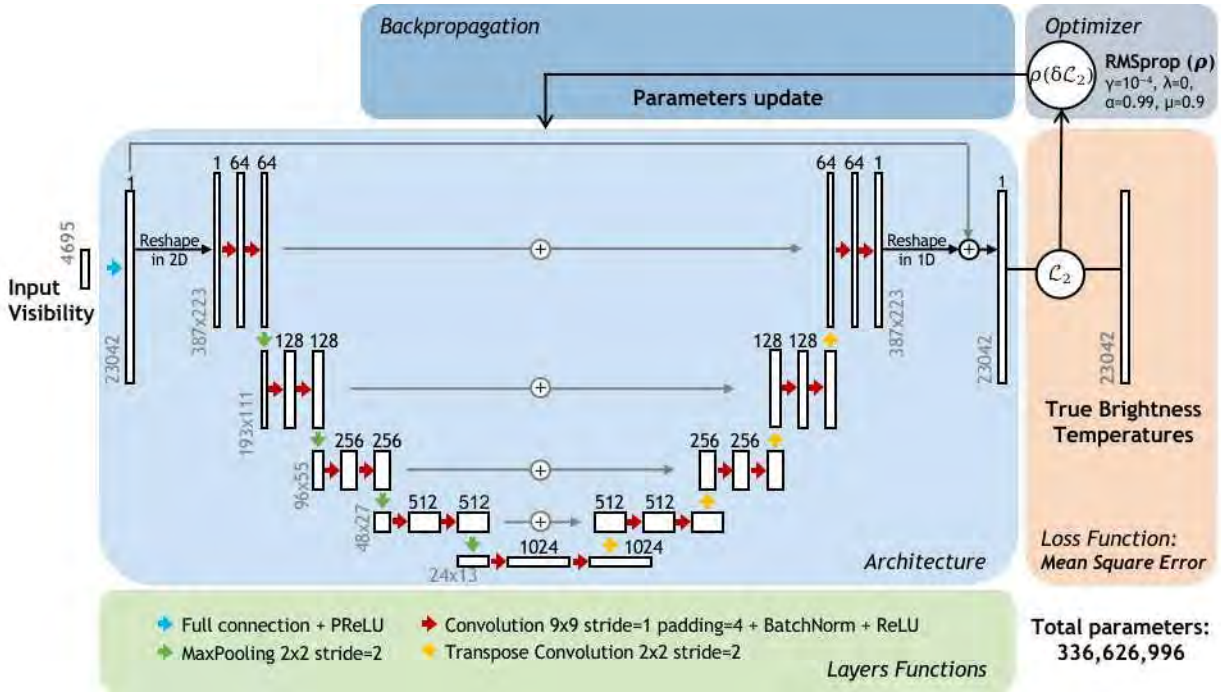
# A deep-learning approach

## DNN architecture

The result of several trials...

Loss function: **MSE**.

A total of **336 million** parameters.

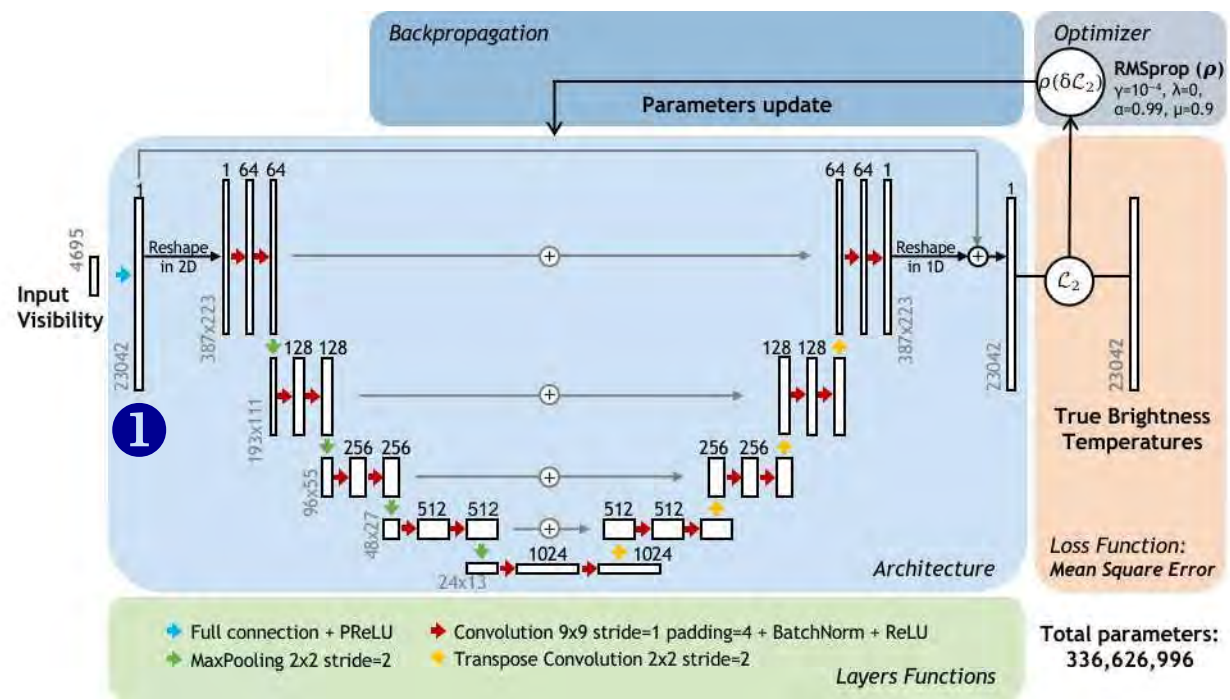




# A deep-learning approach

## DNN architecture

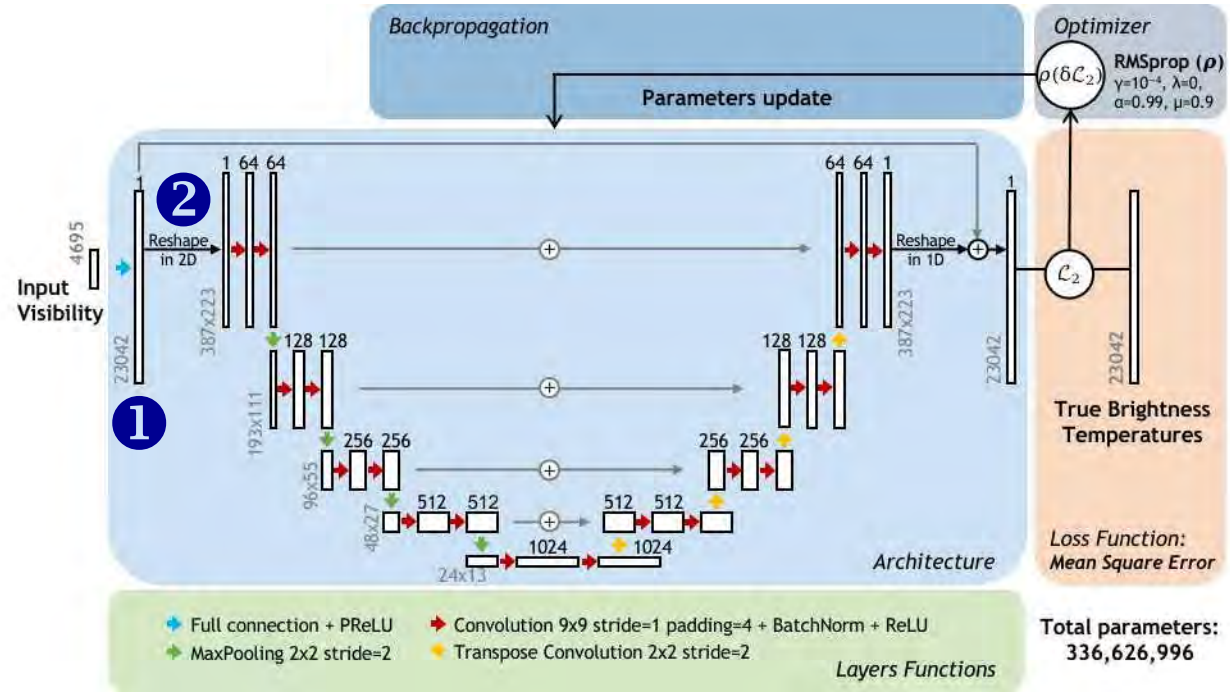
1 fully connected layer: raw inversion of visibilities  
 $4695 V_{pq} \rightarrow 23042 T_{ij}$



# A deep-learning approach

## DNN architecture

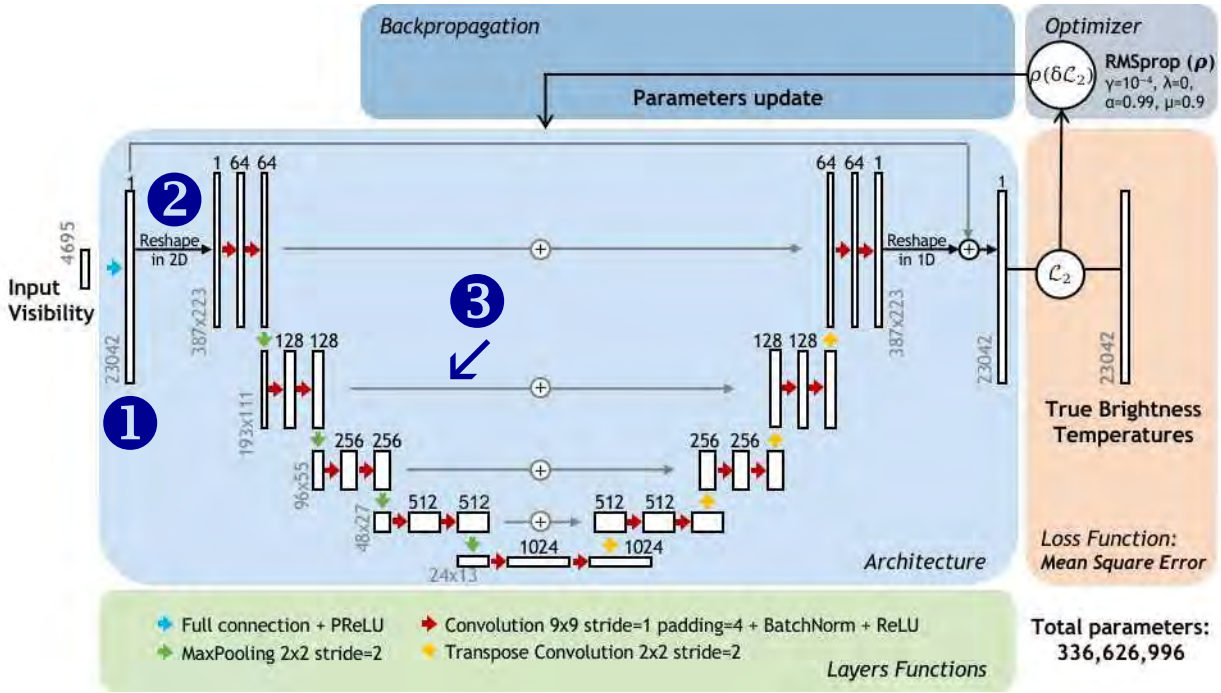
- fully connected layer: raw inversion of visibilities
- reshaped into a 2D sparse regular grid 387x223



# A deep-learning approach

## DNN architecture

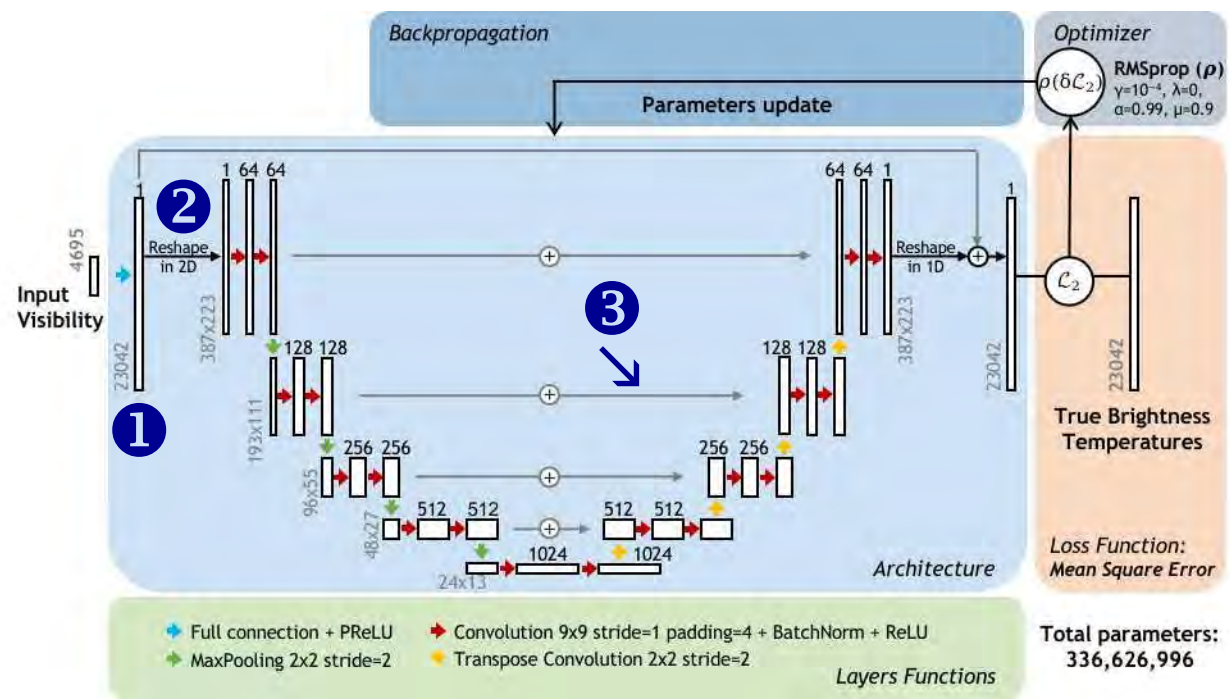
- 1 fully connected layer: raw inversion of visibilities
- 2 reshaped into a 2D sparse regular grid 387x223
- 3 contracting path: sampling  $\div 2$ , feature maps  $\times 2$



# A deep-learning approach

## DNN architecture

- 1 fully connected layer: raw inversion of visibilities
- 2 reshaped into a 2D sparse regular grid 387x223
- 3 expansive path: sampling  $\times 2$ , feature maps  $\div 2$

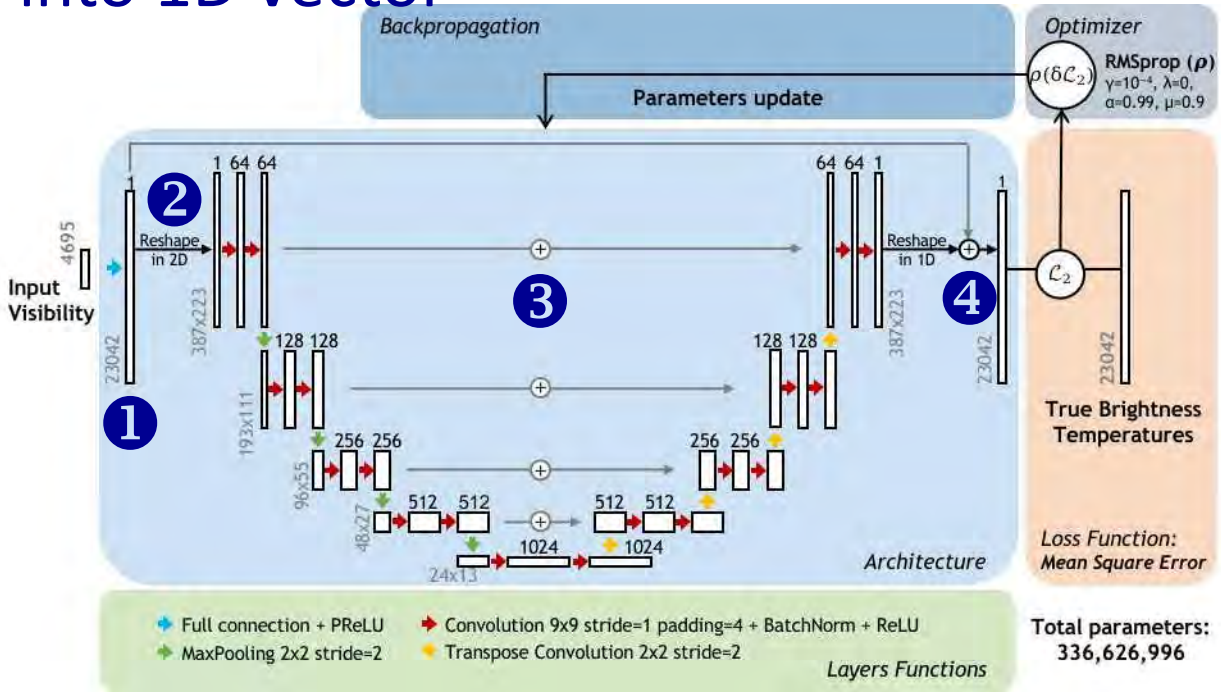




# A deep-learning approach

## DNN architecture

- 1 fully connected layer: raw inversion of visibilities
- 2 reshaped into a 2D sparse regular grid
- 3 contracting/expansive path
- 4 reshape into 1D vector



# A deep-learning approach

## ➤ Training+Validating

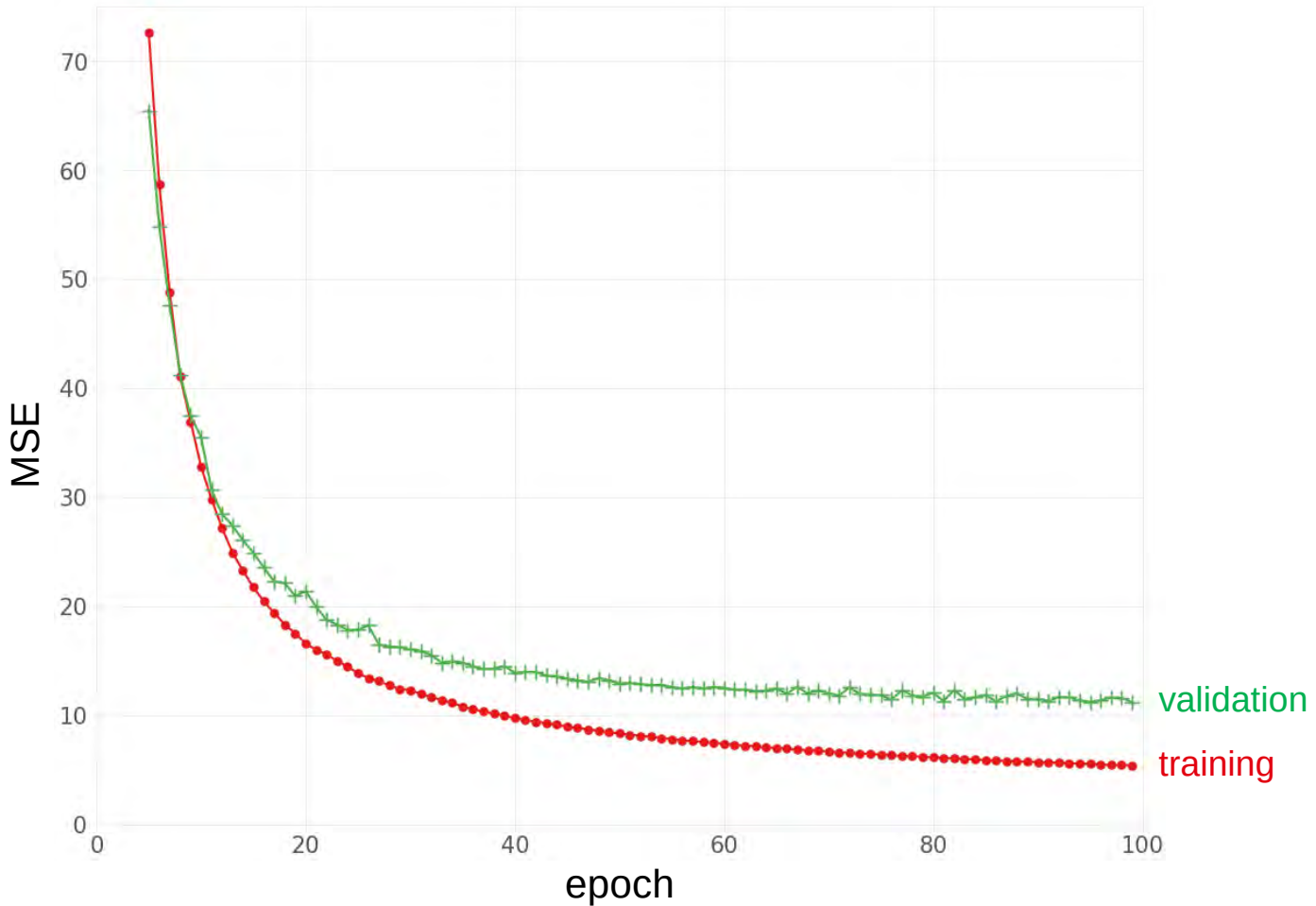
Model trained over 100 epochs  
with mini-batch sizes set to 32  
implemented in Python using PyTorch V1.8.

Training 99774 {T,V} + Validating 33257 {T,V} = 182 h  
on two TESLA V100 SXM2 32 Gbytes GPUs.



# A deep-learning approach

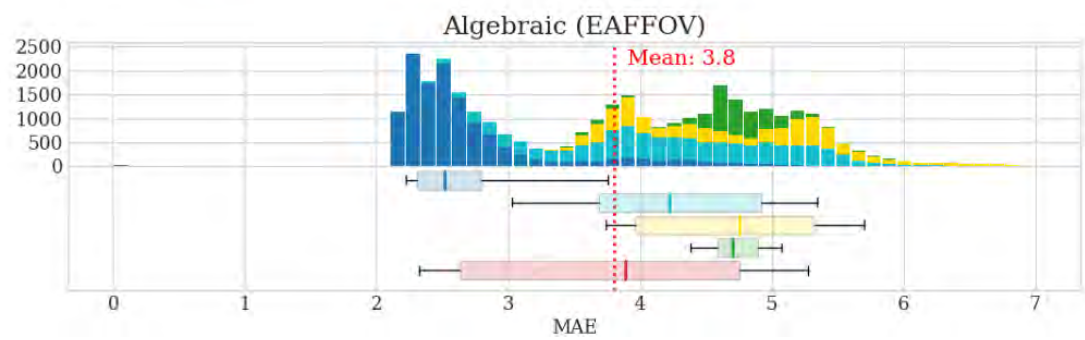
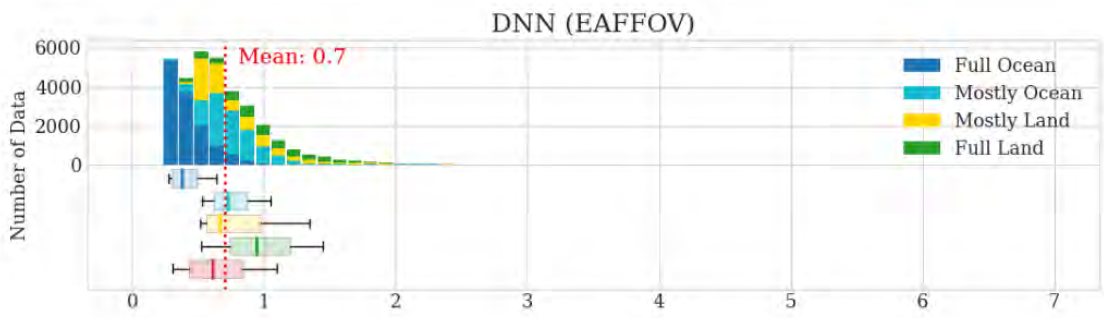
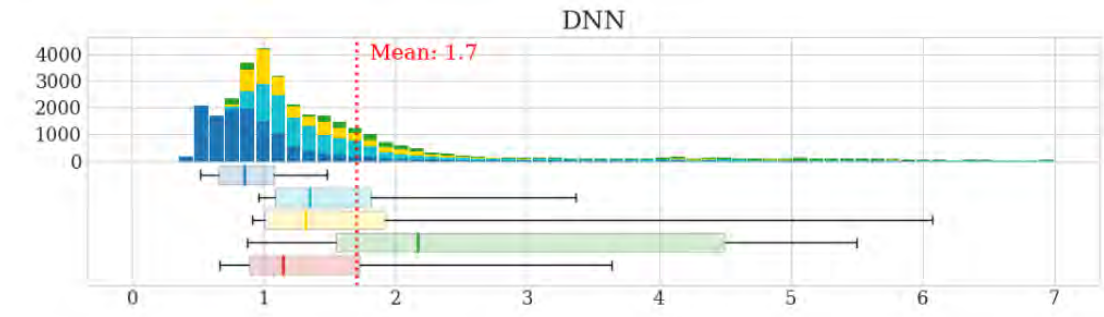
## ➤ Training+Validating: convergence





# A deep-learning approach

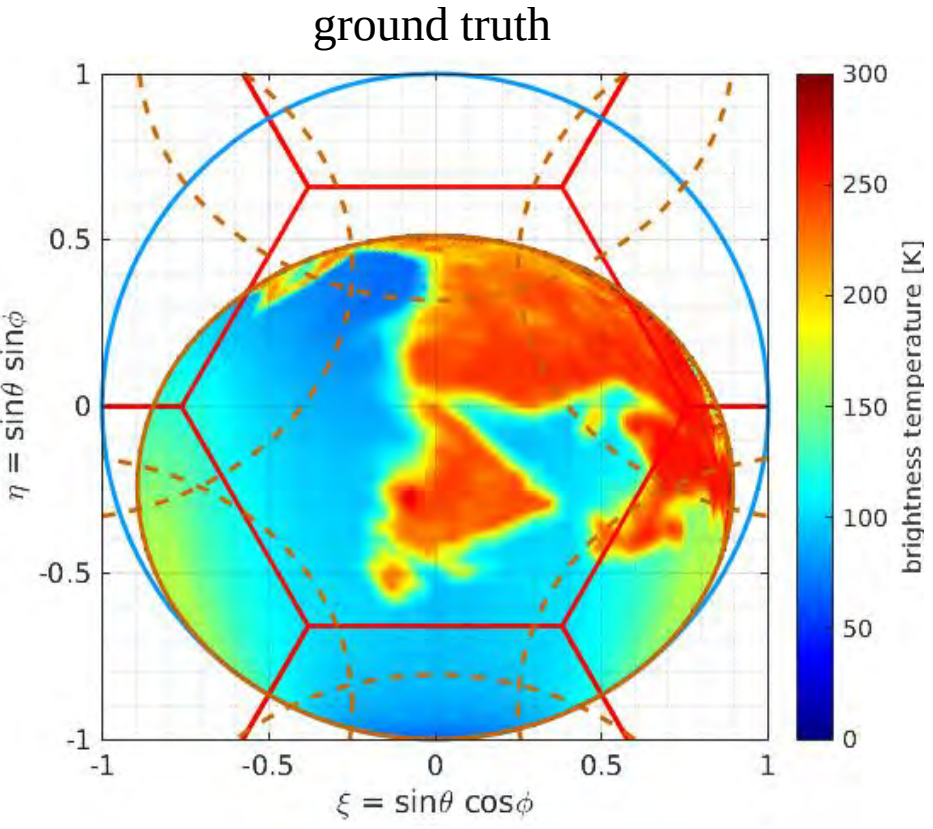
## Testing: reconstructions performances (K-means split)





# A deep-learning approach

## Testing: representative example



average errors  
(entire testing subset)

	MAE	RMSE
DNN (fullFOV)	1.53 K	2.90 K
DNN (EAFFOV)	0.70 K	0.98 K
ALG (EAFFOV)	3.75 K	7.78 K

*This example representative of DNN average MAE over fullFOV*

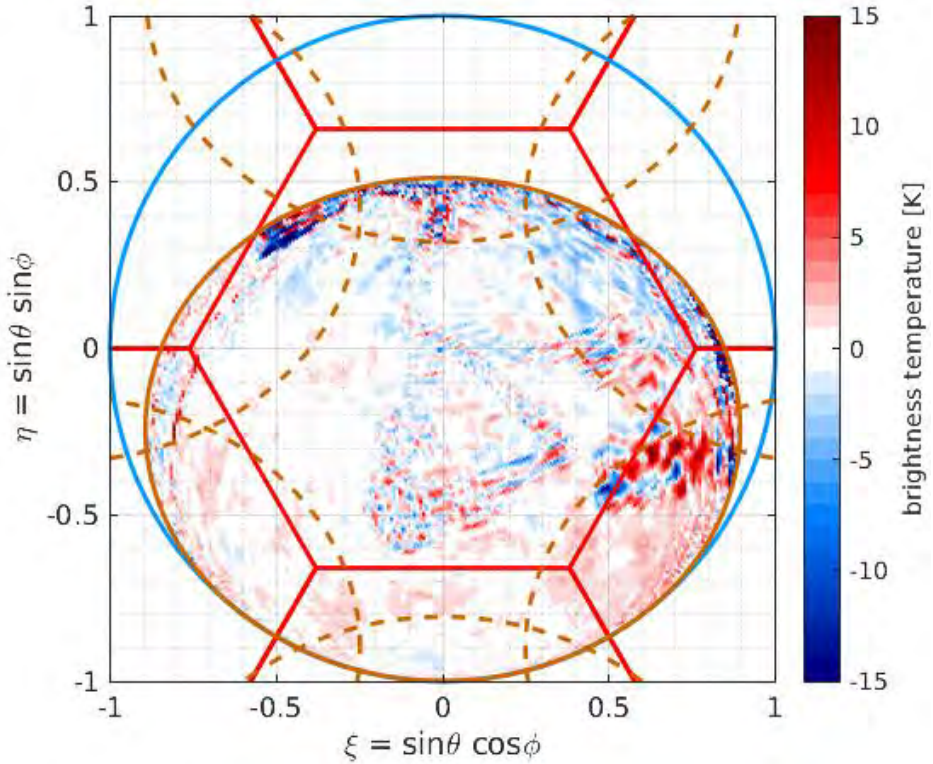
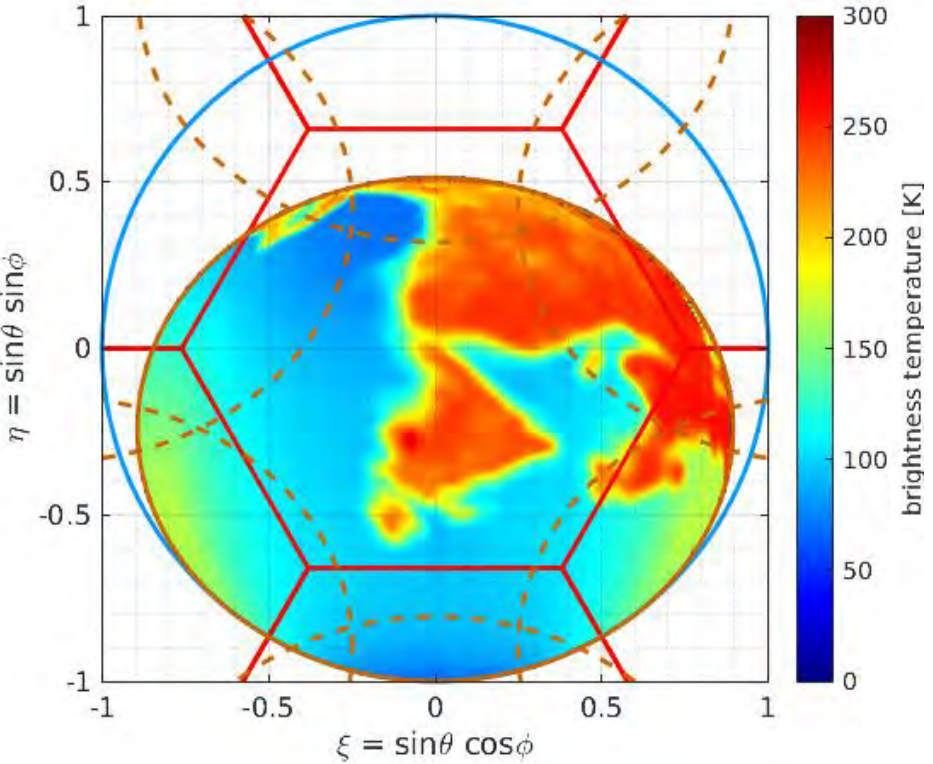
# A deep-learning approach

## Testing: representative example

DNN reconstruction

MAE = 1.5 K (fullFOV)

MAE = 1.0 K (EAFFOV only)

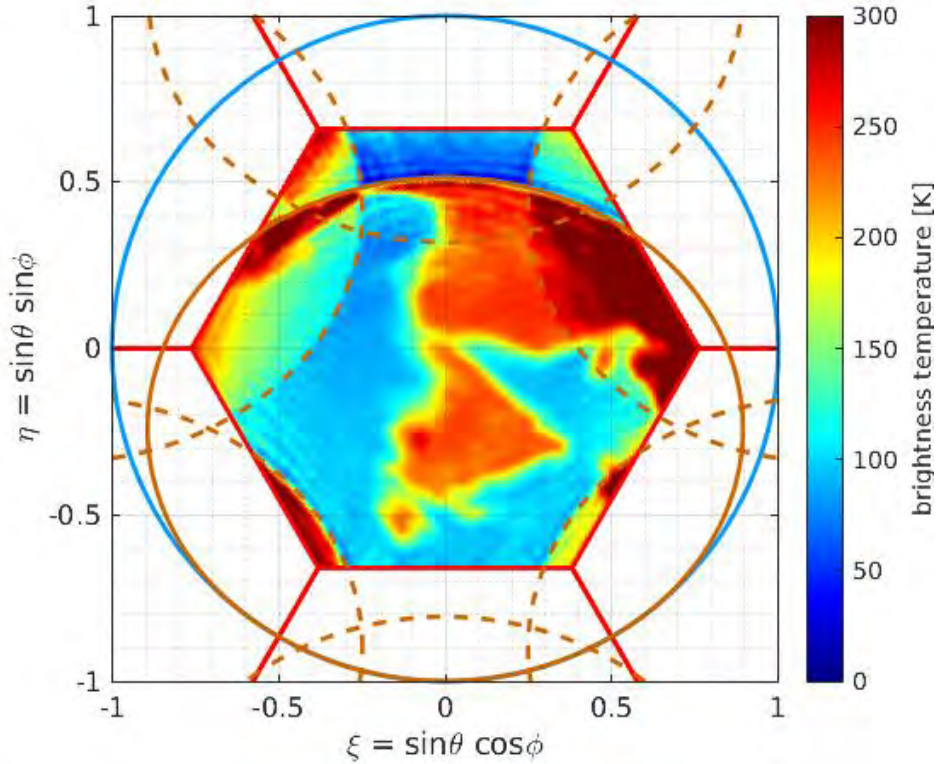


*This example representative of DNN average MAE over fullFOV*

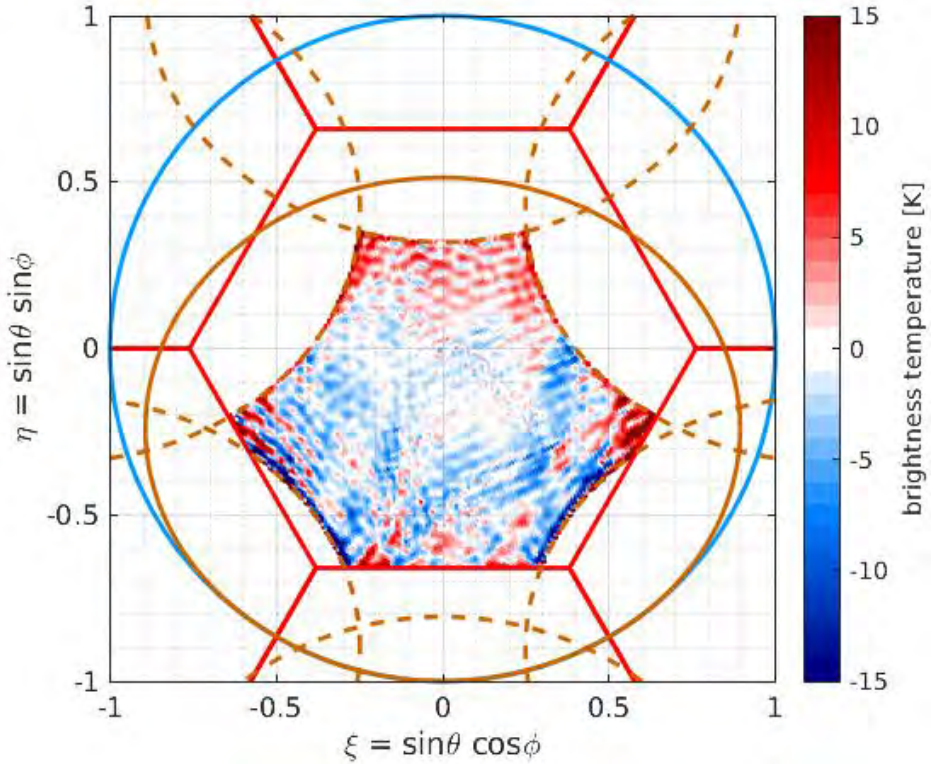
# A deep-learning approach

➤ *Testing: representative example*

ALG reconstruction



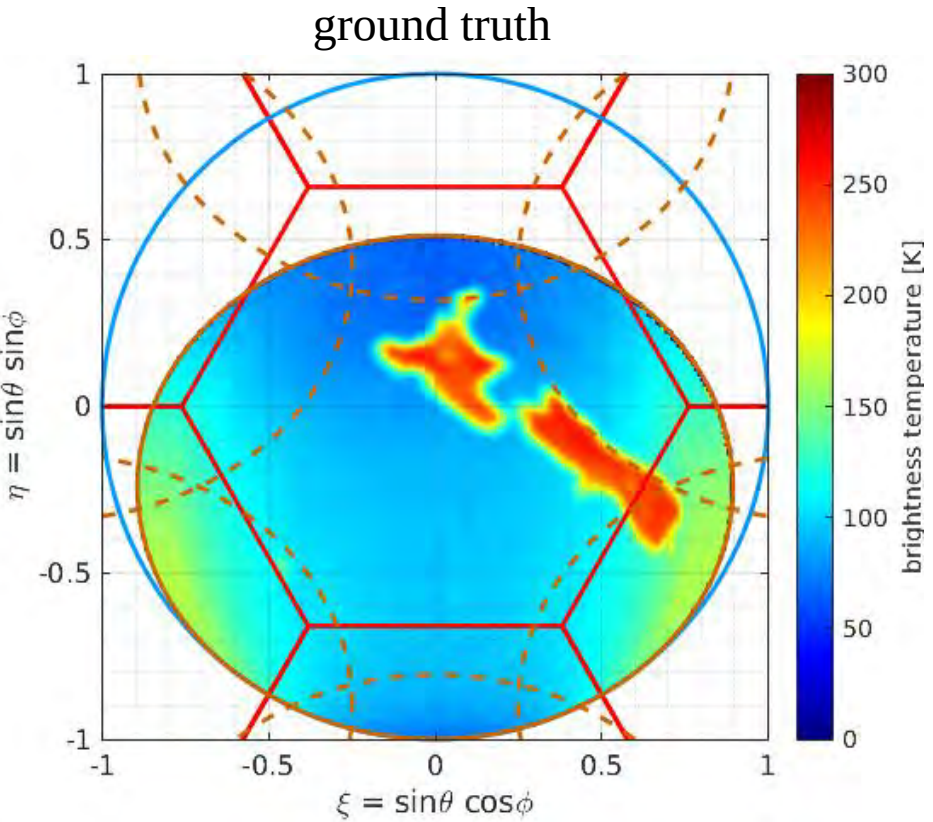
MAE = 3.6 K (EAFFOV only)





# A deep-learning approach

## Testing: representative example



average errors  
(entire testing subset)

	MAE	RMSE
DNN (fullFOV)	1.53 K	2.90 K
DNN (EAFFOV)	0.70 K	0.98 K
ALG (EAFFOV)	3.75 K	7.78 K

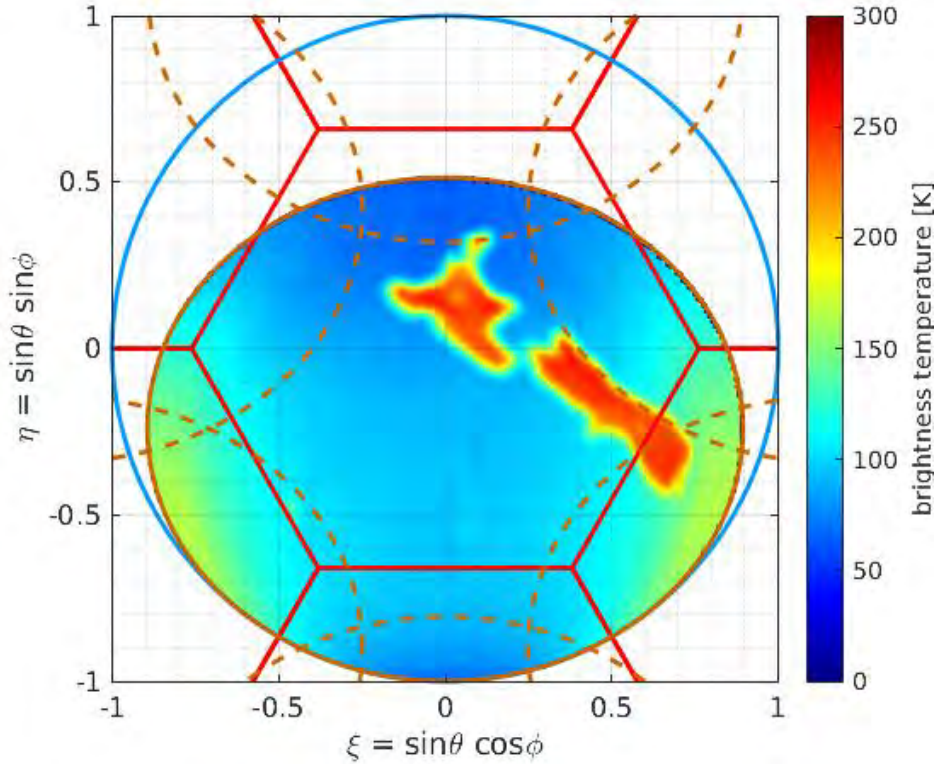
*This example representative of DNN average MAE over EAFFOV*



# A deep-learning approach

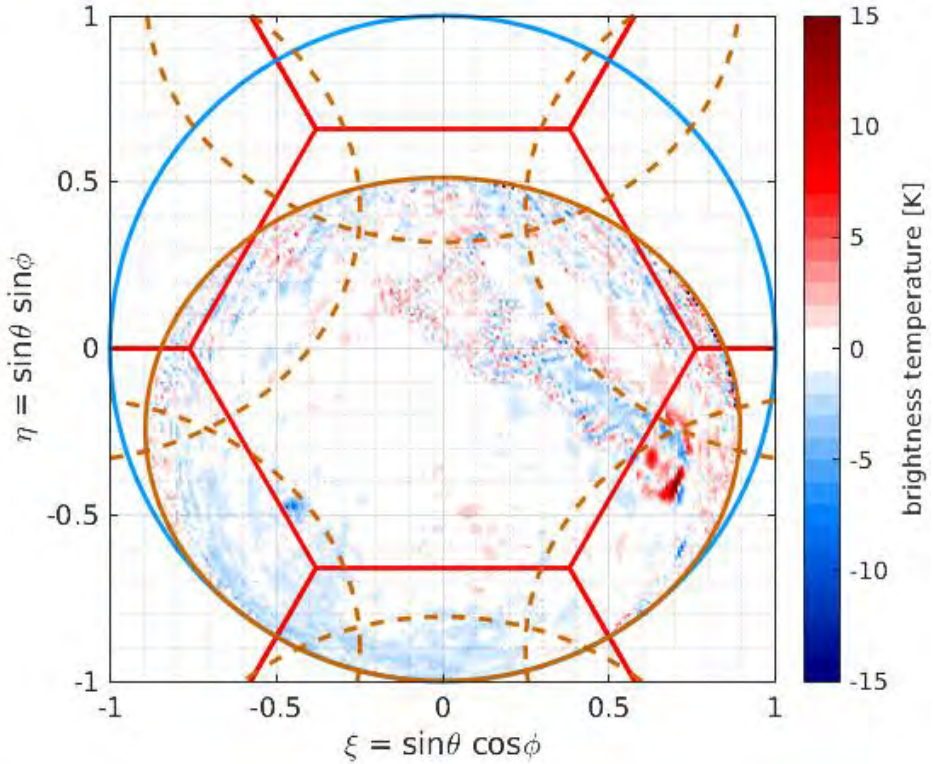
## Testing: representative example

DNN reconstruction



MAE = 0.9 K (fullFOV)

MAE = 0.7 K (EAFFOV only)

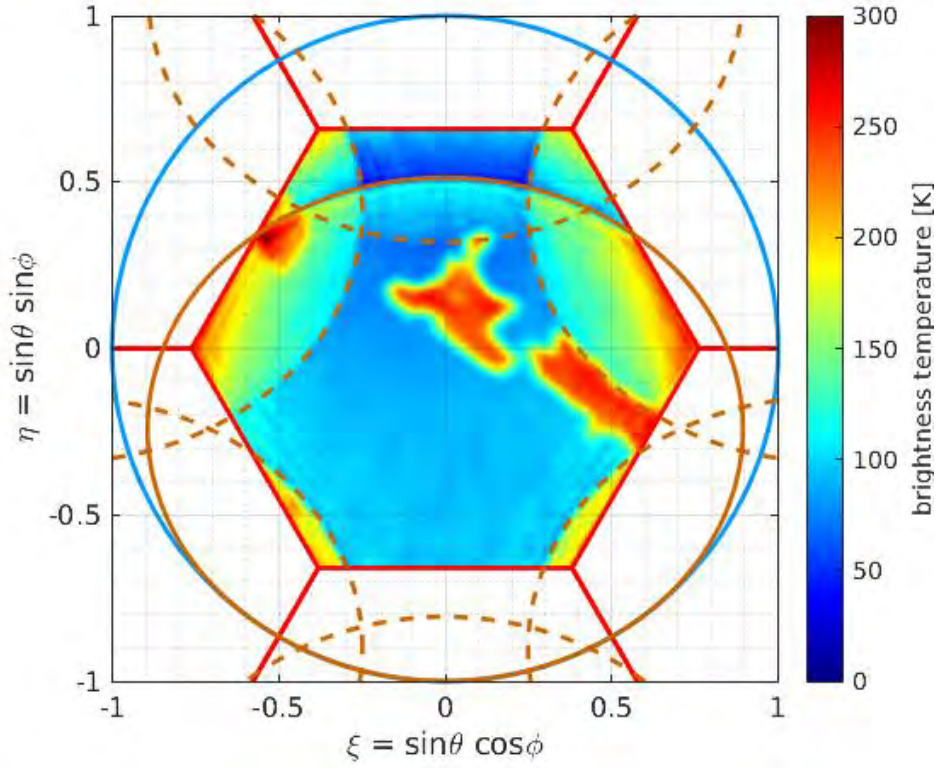


*This example representative of DNN average MAE over EAFFOV*

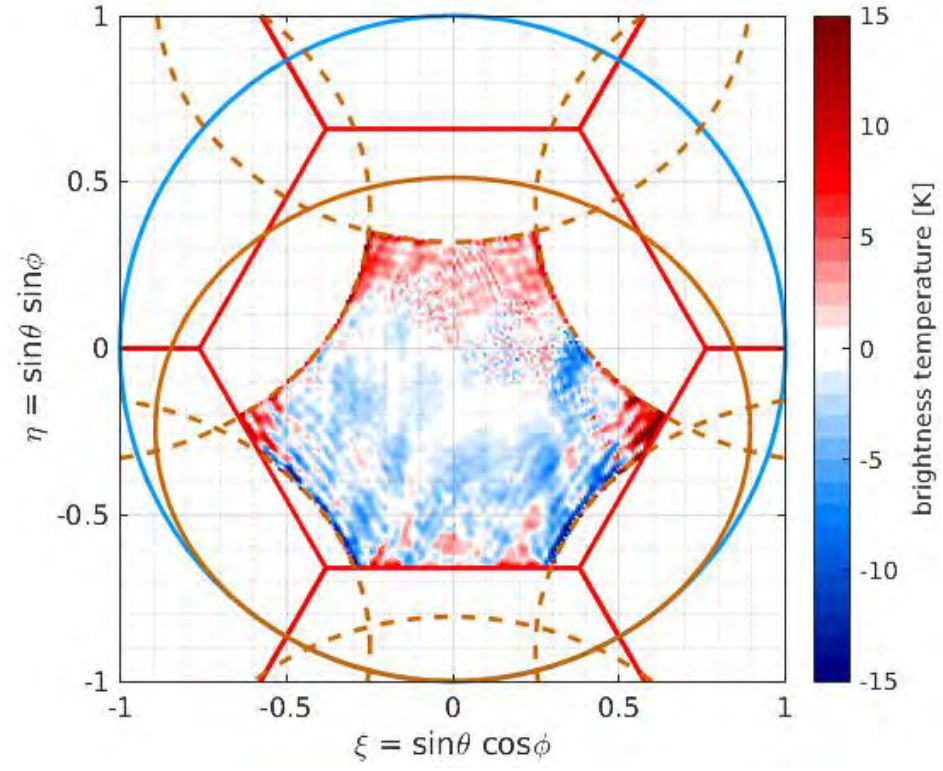
# A deep-learning approach

## Testing: representative example

ALG reconstruction



MAE = 4.3 K (EAFFOV only)

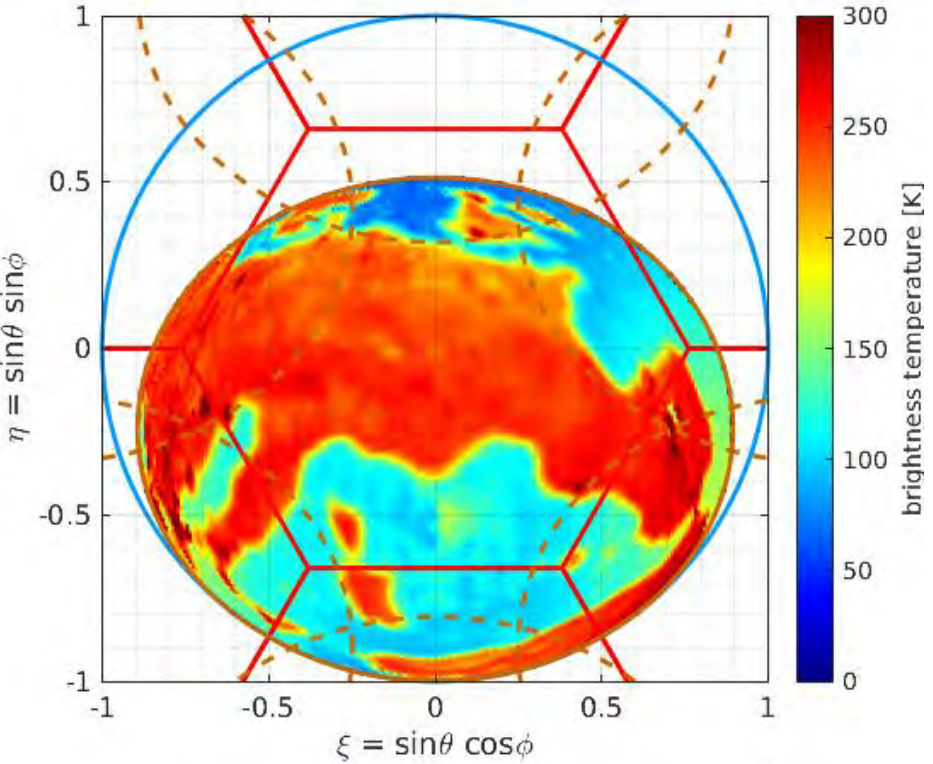




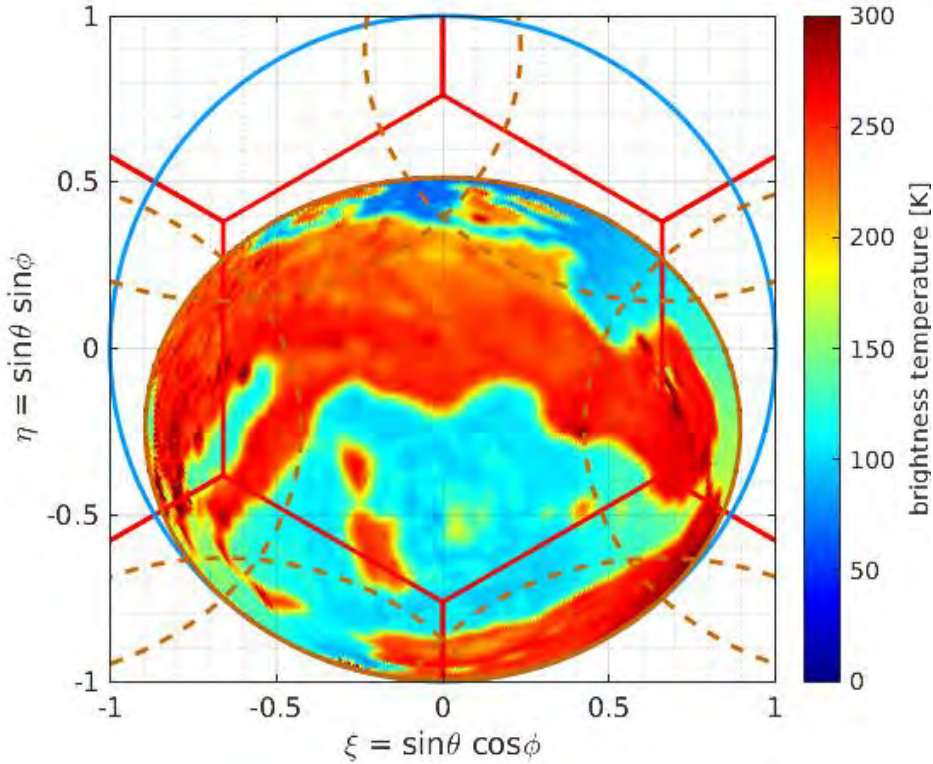
# A deep-learning approach

## Aliases investigations

SMOS  
ground truth



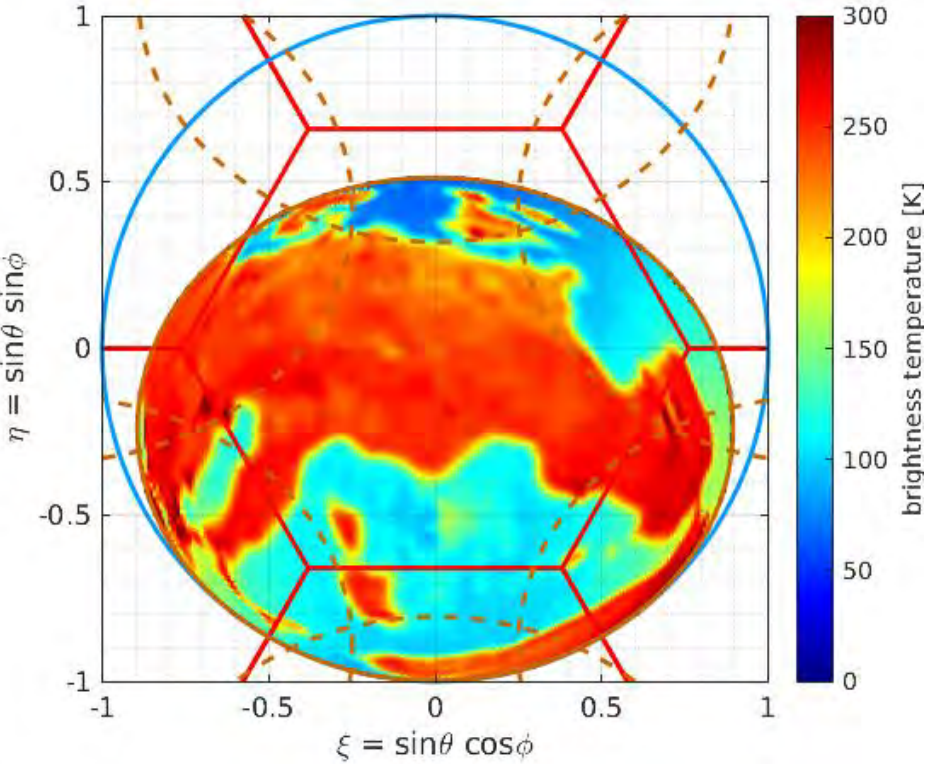
SMOS-90°  
ground truth



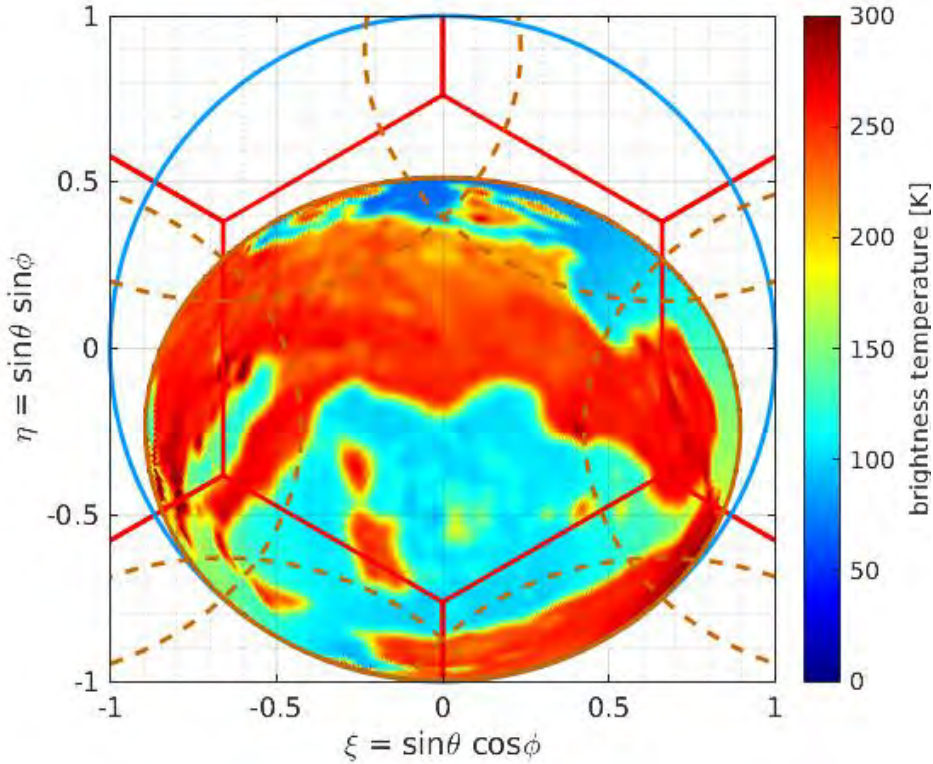
# A deep-learning approach

## Aliases investigations

SMOS  
DNN reconstruction



SMOS-90°  
DNN reconstruction

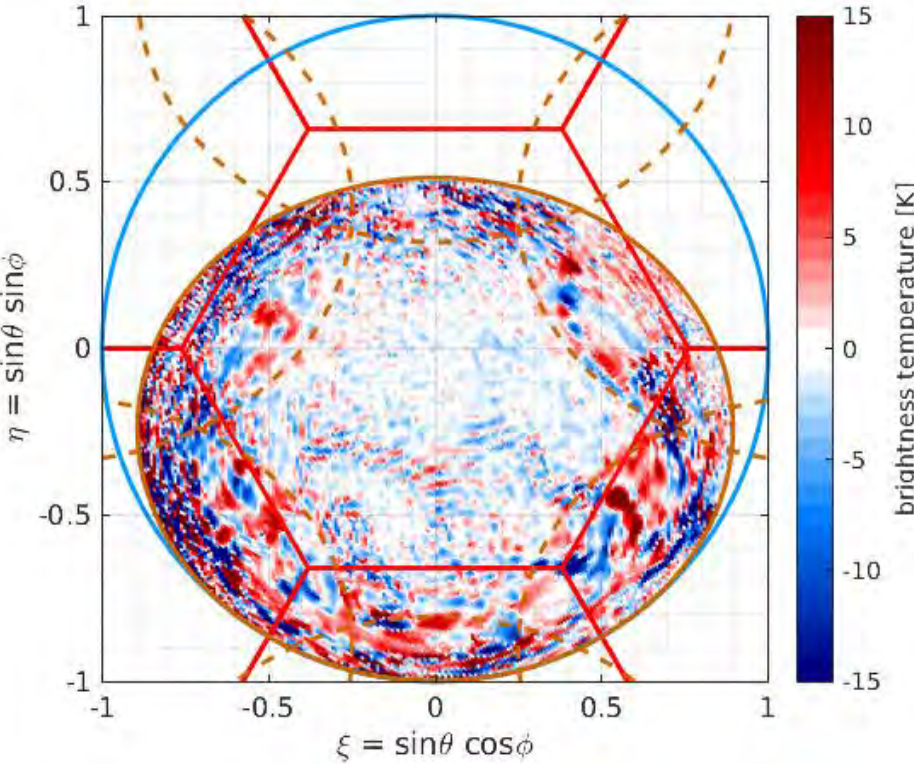




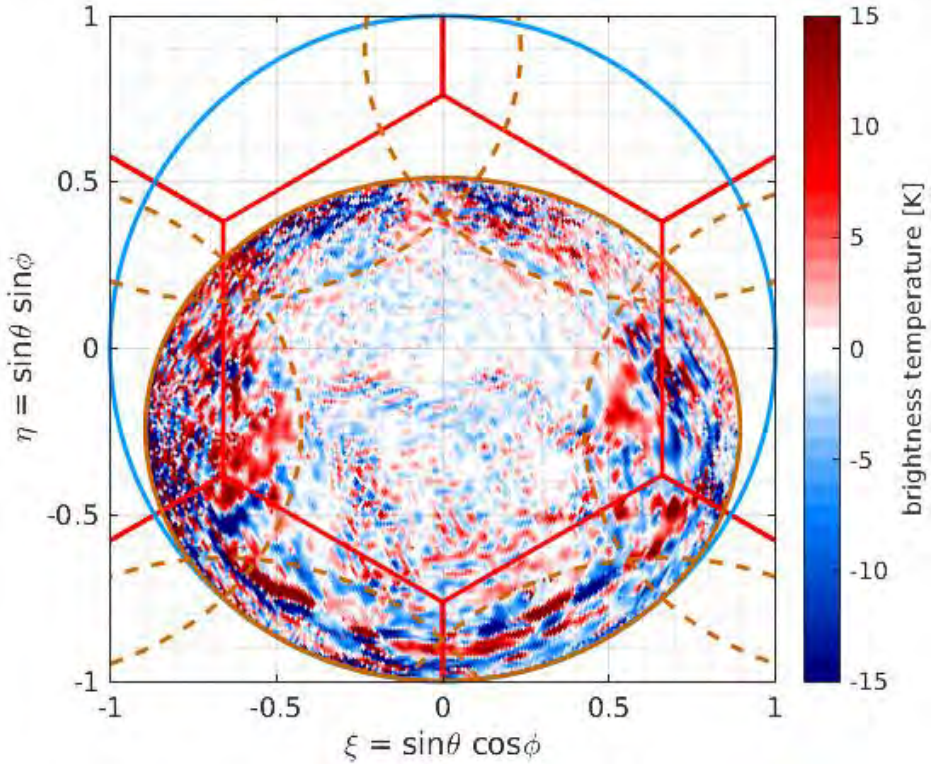
# A deep-learning approach

## Aliases investigations

SMOS  
DNN reconstruction



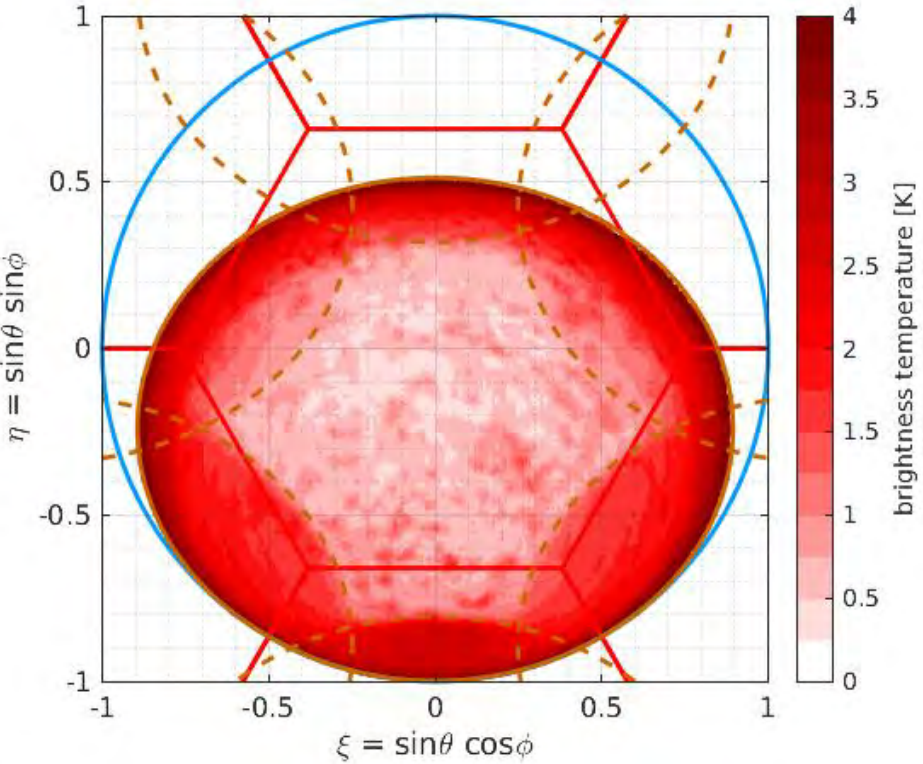
SMOS-90°  
DNN reconstruction



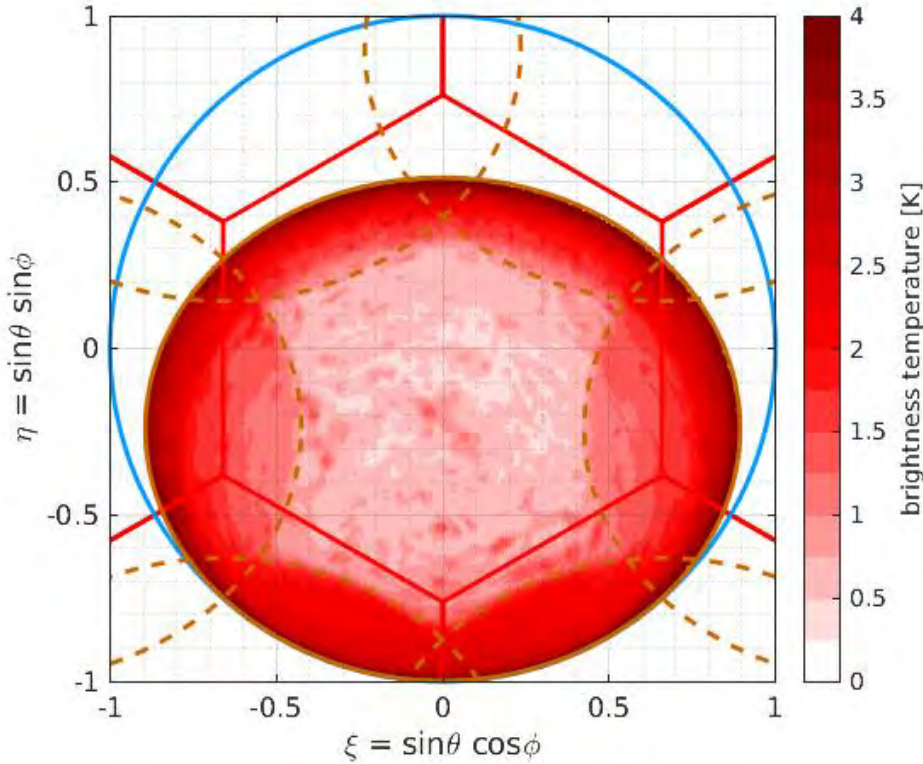
# A deep-learning approach

## Aliases investigations

SMOS  
DNN reconstruction



SMOS-90°  
DNN reconstruction

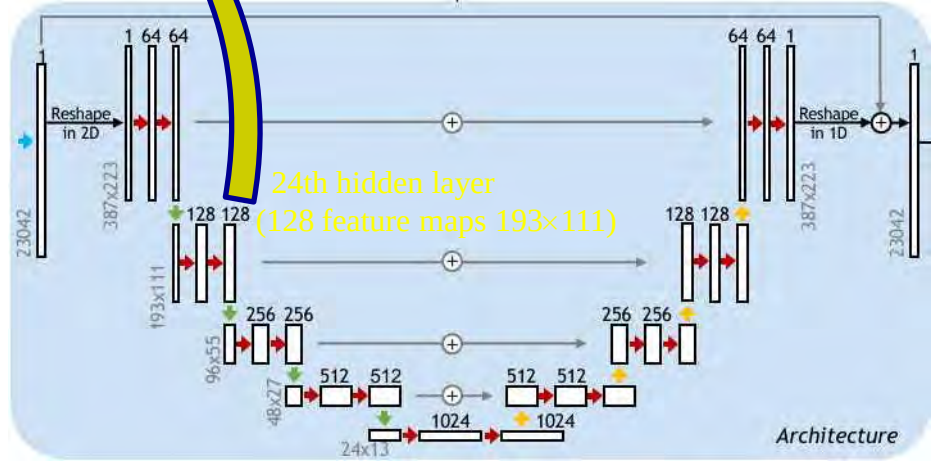
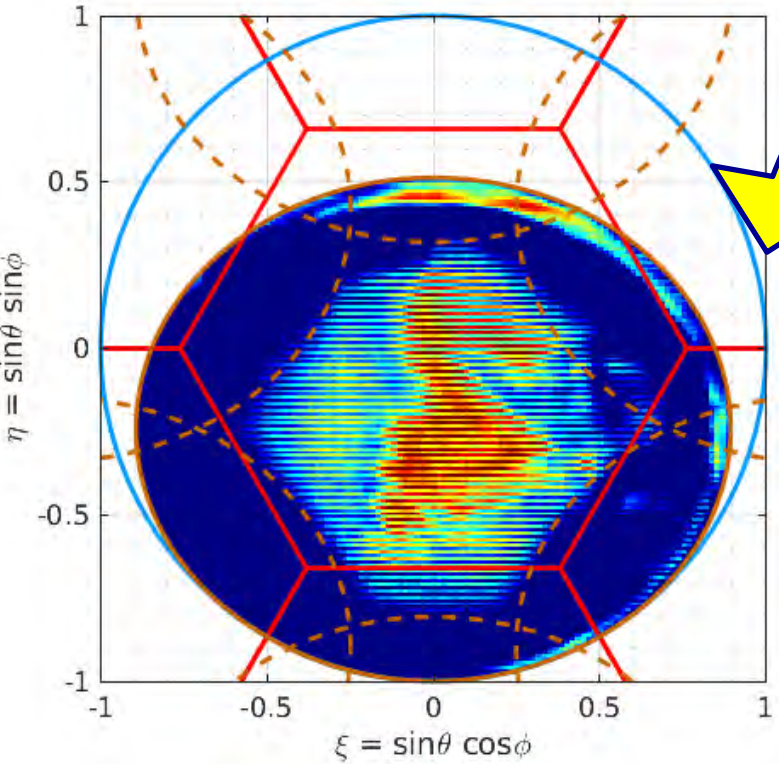




# A deep-learning approach

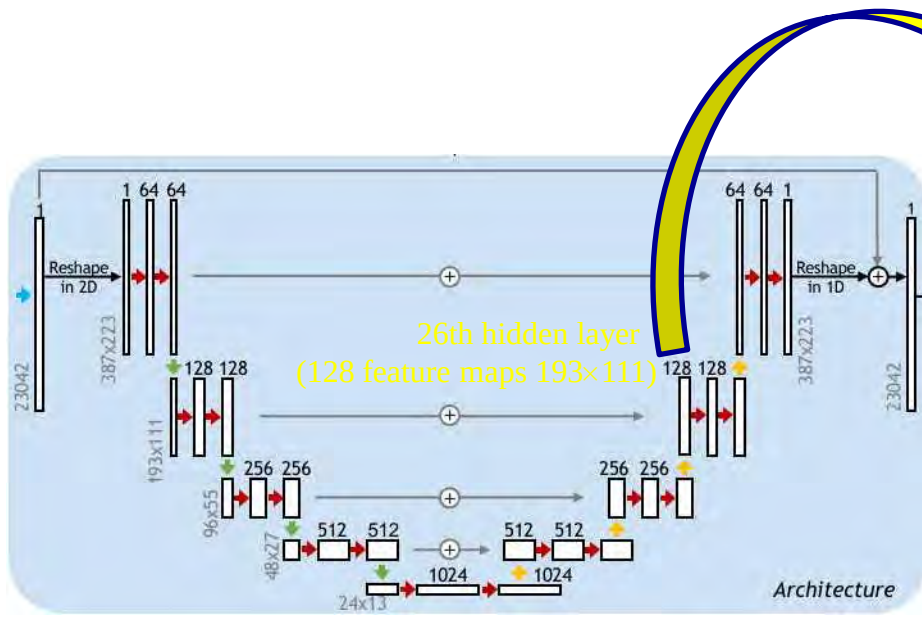
## Hidden layers investigations

neurones activate inside EAFFOV

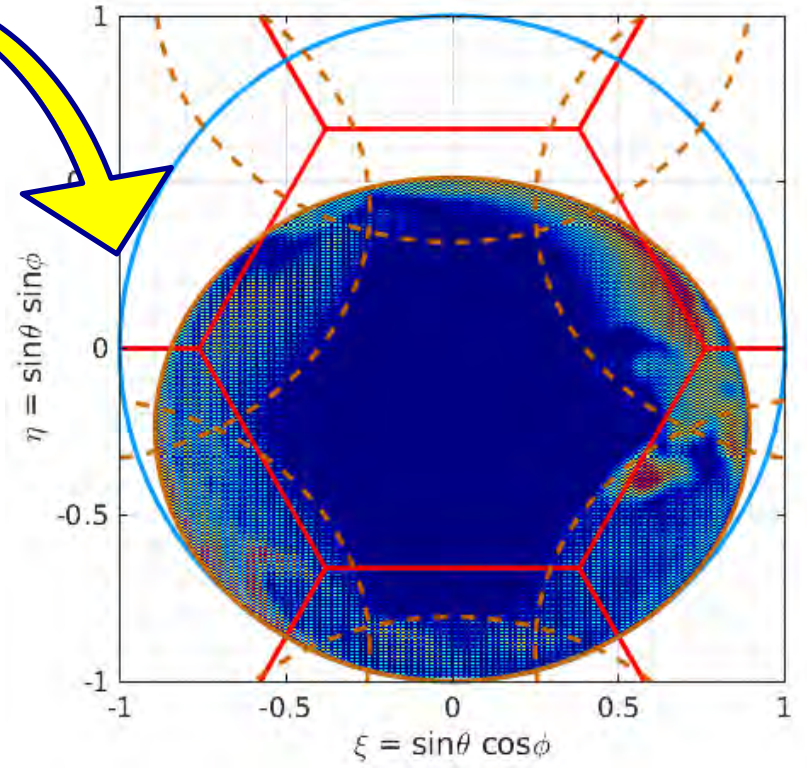


# A deep-learning approach

## ➤ Hidden layers investigations



neurones activate outside EAFFOV





- *The inversion of interferometric data in imaging radiometry has been realized with a Deep Learning approach.*
- *This first experiment has been realized at simulation level: next step is to process SMOS data (on going).*
- ☺ *The main lesson learnt from this first experiment is amazing and very promising for the design of future aperture synthesis radiometers (reduced field aliasing!)*
- ☹ *A long road from idea to (operational) implementation!*
- ☹ *The key role played by training dataset!*
- ☹ *The time/memory necessary for training dataset...*